

NPS ARCHIVE
1966
IMMERMAN, A.

ON THE THERMAL LIMITATIONS
OF DEEP SUBMERGENCE SUBMARINE SHAFT SEALS

by

ARTHUR LESLIE IMMERMAN
LIEUTENANT, UNITED STATES NAVY

B.S., U.S. NAVAL ACADEMY

(1958)

Thesis
I4

MASSACHUSETTS INSTITUTE OF TECHNOLOGY

MAY, 1966

ON THE THERMAL LIMITATIONS
OF DEEP SUBMERGENCE SUBMARINE SHAFT SEALS

by

ARTHUR LESLIE IMMERMAN
B.S., UNITED STATES NAVAL ACADEMY

(1958)

SUBMITTED IN PARTIAL FULFILLMENT

OF THE REQUIREMENTS FOR THE

DEGREE OF MASTER OF SCIENCE

IN MECHANICAL ENGINEERING

AND THE PROFESSIONAL DEGREE,

NAVAL ENGINEER

at the

MASSACHUSETTS INSTITUTE OF

TECHNOLOGY

June, 1966

ON THE THERMAL LIMITATIONS
OF DEEP SUBMERGENCE SUBMARINE SHAFT SEALS

by ARTHUR LESLIE IMMERMEN

Submitted to the Departments of Mechanical Engineering and Naval Architecture and Marine Engineering on 20 May 1966, in partial fulfillment of the requirements for the Master of Science Degree in Mechanical Engineering and the Professional Degree, Naval Engineer.

ABSTRACT

The object of this work is to formulate an analytical model of the heat transfer phenomena in deep submergence submarine shaft seals. It is expected that this will prove useful to design engineers in determining materials and arrangement specifications for these seals.

Interfacial temperature data derived from a comprehensive experimental investigation is compared with thermal results computed from a lumped model of the shaft seal. This latter analytical data is obtained by first defining the model, then calculating the heat source component inputs, and finally utilizing an IBM 7094 computer to aid in solution of the resulting mathematical entanglements.

It was found that the most significant factor in the overall heat transfer scheme is the quantity of bypass cooling water flow. No bypass flow results in an extremely sharp temperature rise with pressure; whereas only a slight amount of flow will reduce the interfacial temperature rise to acceptable levels. It was also found that with a combination of high inlet pressure and low shaft speed, the largest temperature rises were experienced.

It can be concluded that any design change that would limit or eliminate the source of cooling water must be carefully evaluated as to the thermal implications. Further, in any investigation of this nature, due consideration ought to be given to the low-speed/high-pressure limiting condition.

Thesis Supervisor: Herbert Heath Richardson
Title: Associate Professor of Mechanical Engineering

ACKNOWLEDGEMENT

The author wishes to acknowledge the assistance and council of those engineers and technicians of the Friction and Wear Division of the United States Navy Marine Engineering Laboratory at Annapolis, Maryland, who gave their time and patience to introduce the subject of and explain the need for this investigation. In particular, sincere thanks to Mr. Watt Smith and Mr. Ralph Snapp for the initial impetus and their learned technical assistance; and to Mr. Leroy Durkan for his proficient assistance in instrumentation and calibration. Warm appreciation is accorded Mr. Francis Fritag for expert craftsmanship demonstrated while assisting the author in preparation of the test seal ring.

The author also wishes to take this opportunity to express deep appreciation and thanks to Professor Herbert Heath Richardson, the Supervisor of this thesis, for his thought-provoking suggestions and recommendations and warm and friendly assistance throughout.

This work was done in part at the Computation Center at the Massachusetts Institute of Technology, Cambridge, Massachusetts.

TABLE OF CONTENTS

| | <u>Page</u> |
|--|-------------|
| Abstract | 11 |
| Acknowledgement | 111 |
| List of Figures | v |
| Notation | vii |
| CHAPTER | |
| I Introduction | 1 |
| II Experimental Procedure | 4 |
| III Analytical Procedure | 13 |
| IV Results | 29 |
| V Discussion of Results | 43 |
| VI Conclusions and Recomendations | 46 |
| APPENDIX | |
| A Determination of Thermal Resistances | 48 |
| B Computational Procedure | 51 |
| C Bibliography | 56 |

LIST OF FIGURES

| <u>Figure</u> | <u>Title</u> | <u>Page</u> |
|---------------|--|-------------|
| I | Submarine Shaft Seal | 2 |
| II | Seal Ring Photograph | 5 |
| III | Pressure Taps | 6 |
| IV | Thermocouples | 7 |
| V | Test Seal Installation Photograph | 8 |
| VI | Test Rig Photograph | 9 |
| VII | Instrumentation Photograph | 11 |
| VIII | Seal Face Profiles | 12 |
| IX | Estimated Thermal Resistances | 14 |
| X | Pressure Profile Range (2000 psi) | 16 |
| XI | " " " (1500 psi) | 17 |
| XII | " " " (1000 psi) | 18 |
| XIII | " " " (500 psi) | 19 |
| XIV | " " " (300 psi) | 20 |
| XV | " " " (200 psi) | 21 |
| XVI | Balance Pressure & Seal Face Flow | 23 |
| XVII | Seal Face Clearance | 25 |
| XVIII | Coefficient of Friction | 27 |
| XIX | Heat Input vs. Pressure | 28 |
| XX | Seal Face Temperature vs. Heat Input | 30 |
| XXI | Seal Face Temp. vs. Pressure ($Q_b=0.0$) | 31 |
| XXII | Seal Face Temp. vs. Pressure ($Q_b=0.1$) | 32 |

| <u>Figure</u> | <u>Title</u> | <u>Page</u> |
|---------------|-----------------------------------|-------------|
| XXIII | "T" vs. " Q_b " - (p = 200 psi) | 33 |
| XXIV | " (p = 300 psi) | 34 |
| XXV | " (p = 500 psi) | 35 |
| XXVI | " (p = 1000 psi) | 36 |
| XXVII | " (p = 1500 psi) | 37 |
| XXVIII | " (p = 2000 psi) | 38 |
| XXIX | " (p = 2000 psi) | 39 |
| XXX | " (p = 3000 psi) | 40 |
| XXXI | " (p = 4000 psi) | 41 |
| XXXII | " (p = 5000 psi) | 42 |

NOTATION

| | |
|------------|---|
| A | seal face area |
| c | mean seal clearance |
| C_p | coefficient estimating the net average contact stress |
| f | coefficient of friction |
| G | duty parameter |
| h | surface coefficient of heat transfer |
| J | mechanical equivalent of heat |
| k | thermal conductivity |
| N | rotational speed |
| p | inlet pressure |
| Δp | pressure drop across seal face |
| q | total rate of heat transfer |
| Q_b | bypass coolant flow around the seal |
| Q_f | fluid film flow the seal interface |
| R | mean seal radius |
| t | torque |
| T | non-dimensional temperature |
| T_a | ambient temperature |
| T_f | temperature at seal face |
| U | average linear velocity at seal ring face |
| w | seal face width |
| W | total load supported by the seal face |
| μ | coefficient of viscosity |

I

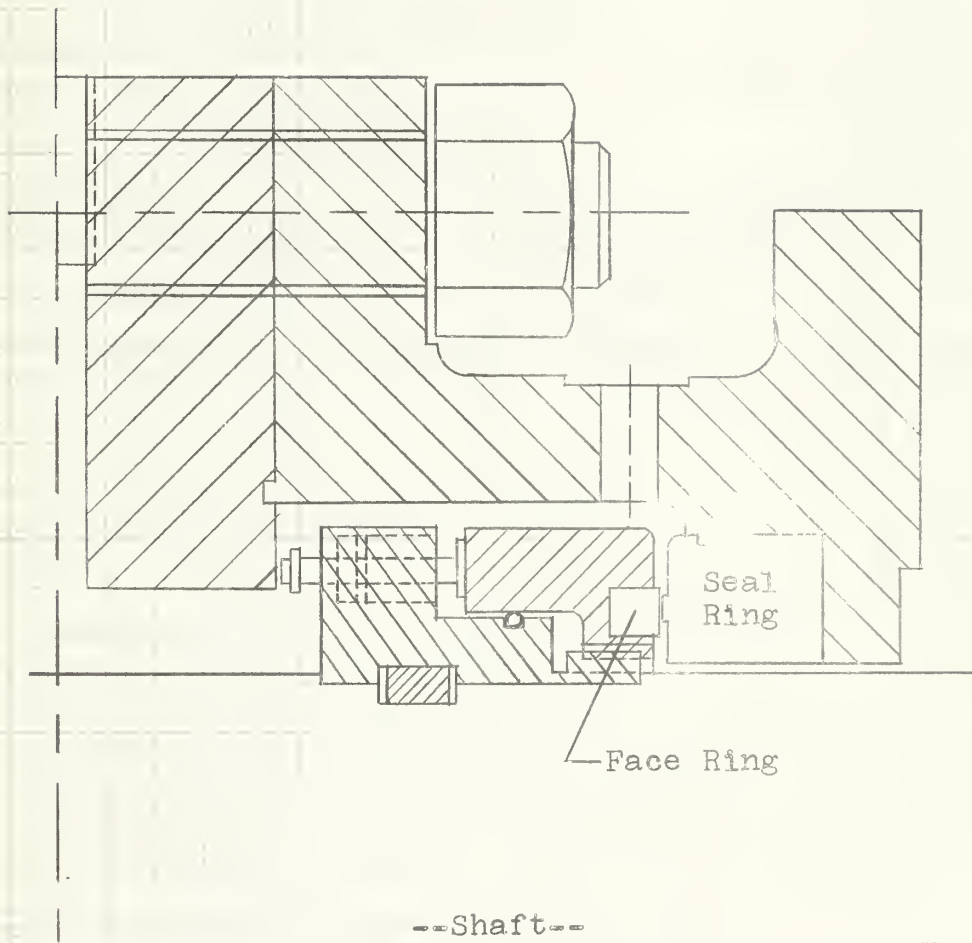
INTRODUCTION

Limitation of the amount of sea water that penetrates the hull of a submarine along the propulsion shafting presents a variety of problems, most of which have been or are being examined.^(1,2,3,4,5) However, one area of interest, in which no experimental work has been done, and little analytical effort has been expended, is in the thermal limitations of submarine shaft seals.^(2,3) The type of shaft seal presently being utilized in submarine design is of a radial face, balanced pressure design with a small amount of leakage flow. (see Figure I) A requirement exists to determine the quantity of heat generated at the seal interface and the efficiency with which this heat can be dissipated.

Up until quite recently, no heat generation or heat dissipation problems were encountered in the design of these seals. This was due to the fact that submarines were designed with an auxiliary salt water piping system in which the pressure was maintained slightly above sea pressure. It was only a secondary purpose of this system to provide positive flow to the shaft seal. This provided a slight amount of leakage through the seal and a large amount of bypass flow overboard. This latter bypass flow served to effectively remove generated heat from the seal. Two conditions have arisen which now make

FIGURE I

SUBMARINE SHAFT SEAL



Note: All material
monel except:
Seal Ring - Beryllium
Face Ring - Tungsten
Carbide

ALI 5/66

the thermal limitations of these seals a problem that must be faced and quantitatively determined. First, the auxiliary salt water system may be completely eliminated in future submarine designs. ⁽⁶⁾ This would effectively remove a major portion of the necessary heat sink of the shaft seals. Further, as submarine designs and operating profiles trend more and more towards deeper submergence, the quantity of heat generated at the seal face grows quite rapidly.

It is the object of this thesis to first present a description of an experimental investigation into the thermal conditions existing in deep submergence submarine shaft seals. Then an analytical model of shaft seal is developed and utilized to formulate a method of predicting maximum interfacial temperatures. In the analysis, some of the variables are determined solely from theory, while the determination of others is based in part on theory and partly on the results of the experimental data. The experimental results are then presented and compared with the analytical results. Extrapolations are made to include conditions beyond the physical capabilities of the test rig.

It is expected that the analytical procedure determined in this paper will be utilized by shaft seal design engineers in material and arrangement specifications, and that a great deal of costly and time consuming experimental work will thereby be avoided.

II

EXPERIMENTAL PROCEDURE

A 5 5/8" shaft diameter test rig for submarine shaft seals was utilized for gathering experimental data. Maximum testing conditions were limited to a pressure of 2000 psi and a rotational speed of 375 rpm.

A bearium seal ring was selected for instrumentation. Bearium (commercial trade name) is a leaded bronze composition that has been found quite suitable for use as a seal ring in submarine shaft seals. (see Figure II) Five 1/64" holes were drilled at equal (0.044") spacings across the 0.263" of the seal ring face. These holes were counter-sunk and fitted with 1/8" copper tubing for further connection to pressure sensing devices. (see Figure III) Holes were drilled for nineteen (19) chrome alumen thermocouples which were then inserted in the seal ring and seated with epoxy. (see Figure IV)

The seal ring face was then lapped and profiled with an X-Y plotter at three separate circumferential positions. The face ring (tungsten carbide) and the seal ring were inserted in the housing and assembly of the test apparatus was completed. (see Figures V and VI) The area ratio (face area of the sealing surface to balance area behind face ring housing) was 0.523. A sealol step seal, for which leakage

FIGURE II

5-5/8" HIGH PRESSURE DEEP SUBMERGENCE SEAL RING

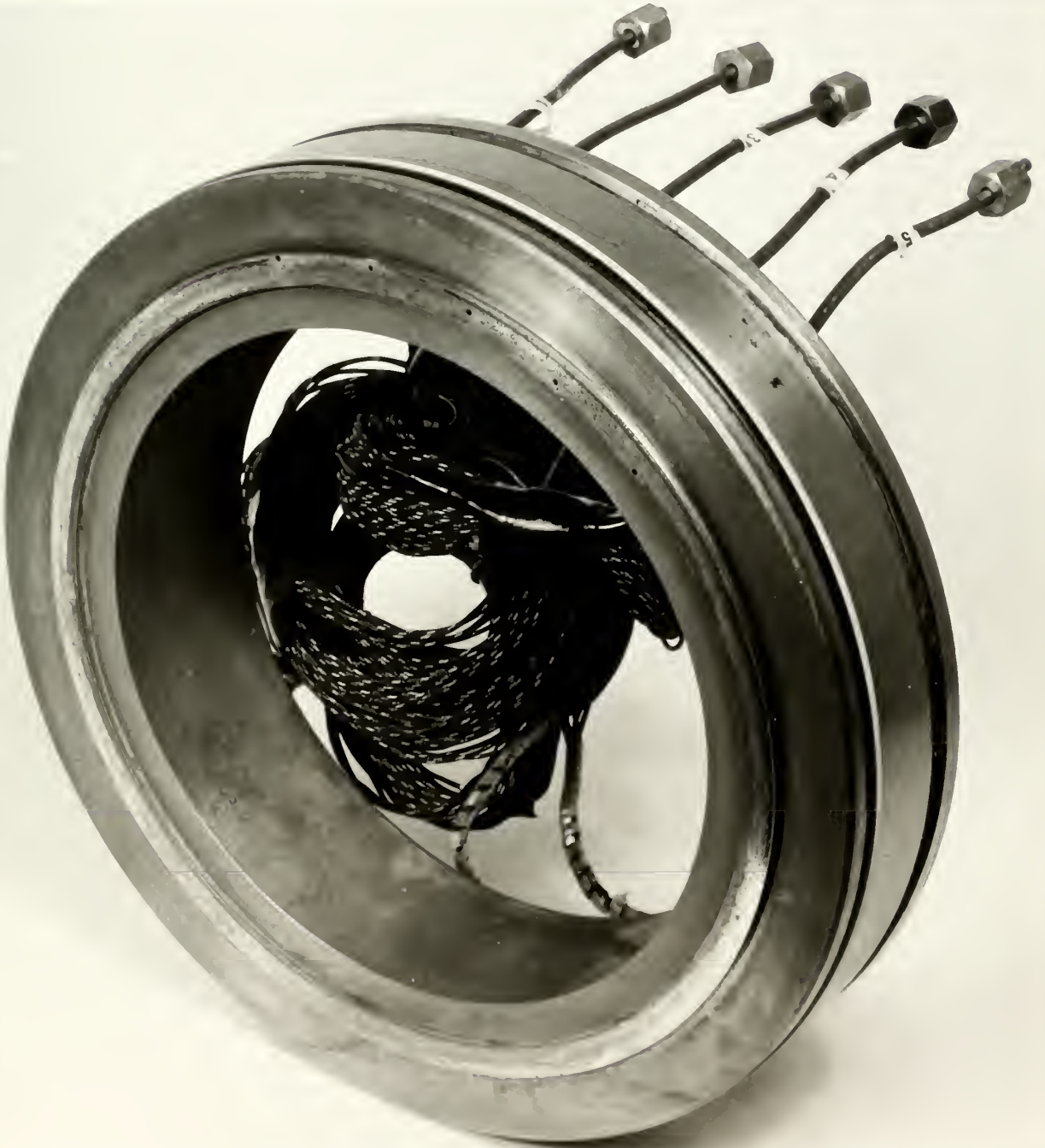
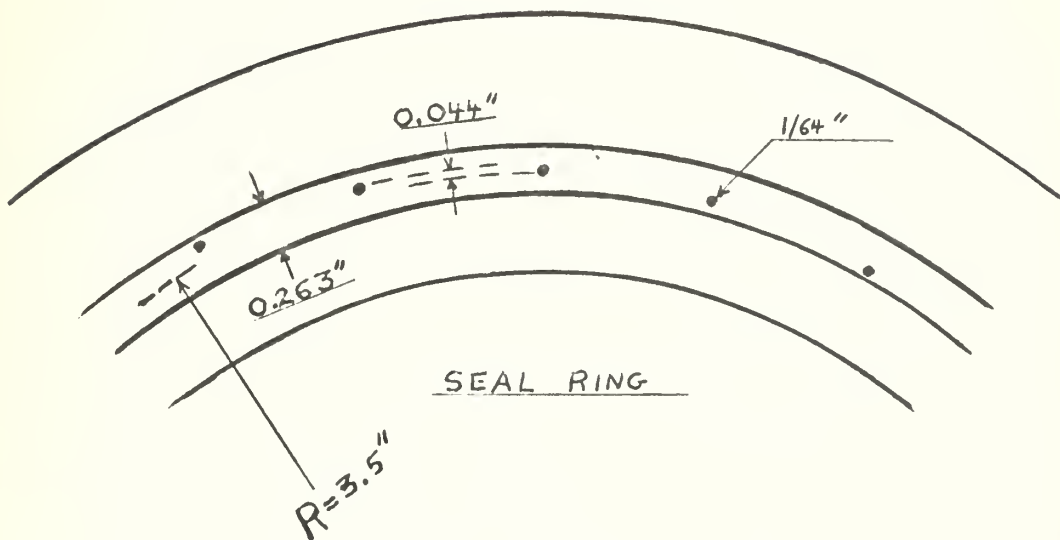


FIGURE III

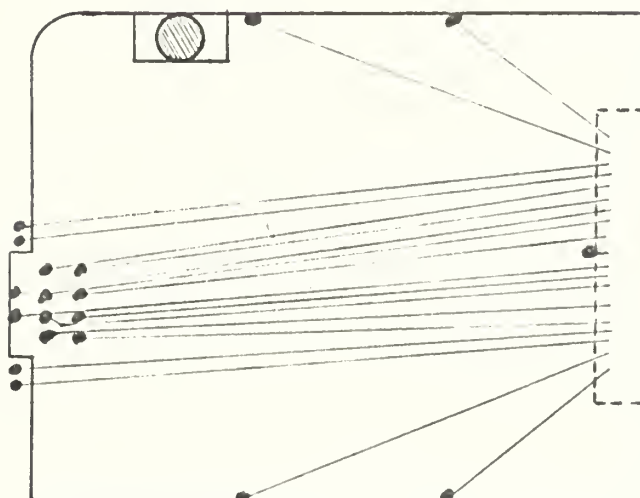
PRESSURE TAPS



SCALE-FULL

FIGURE IV

THERMOCOUPLES



SEAL RING

SCALE: 2" = 1"

- TC CIRCUMFERENTIALLY
SPACED AROUND SEAL RING -

FIGURE V

SEAL RING INSTALLED IN PRESSURE HOUSING
(Thermocouple and Pressure Tap Connections)

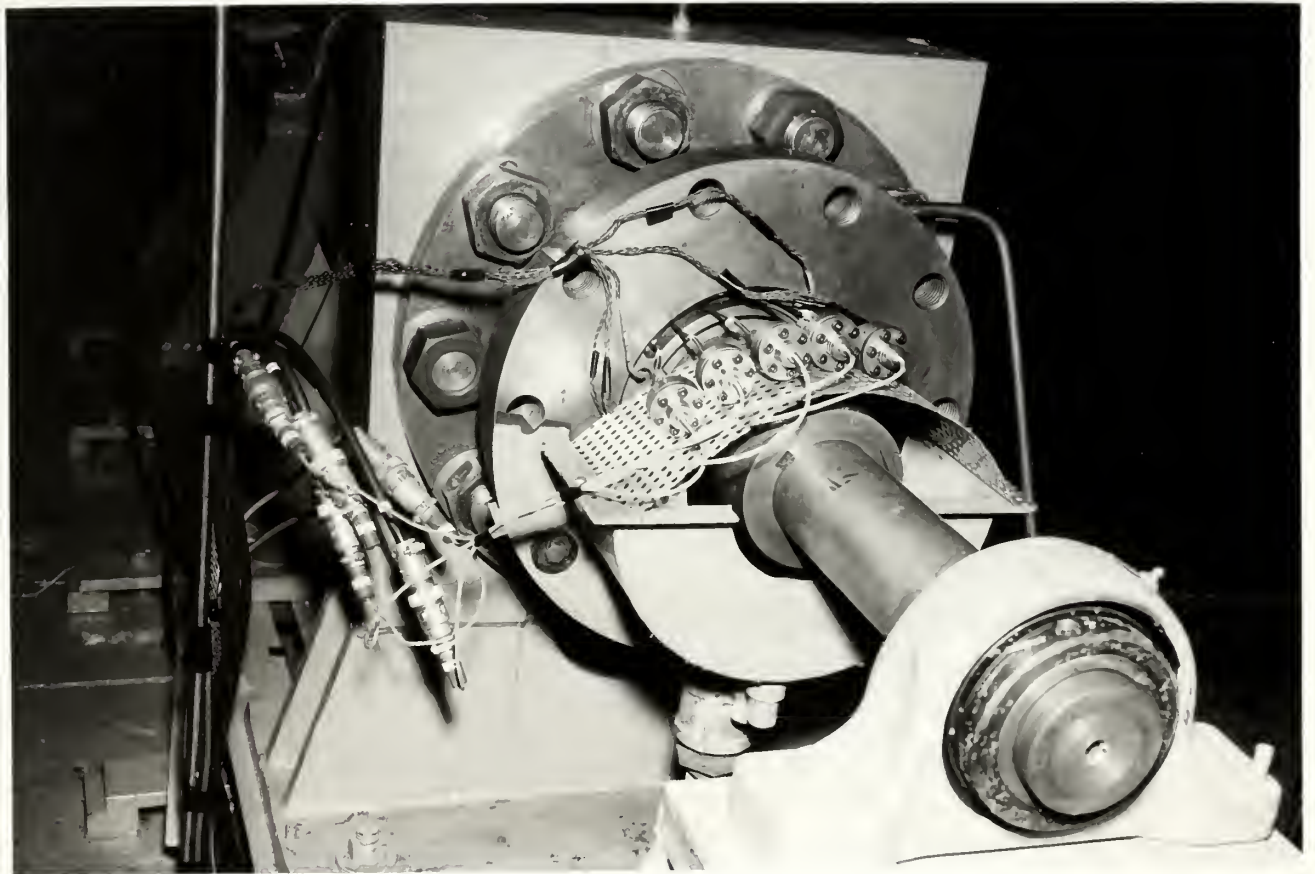
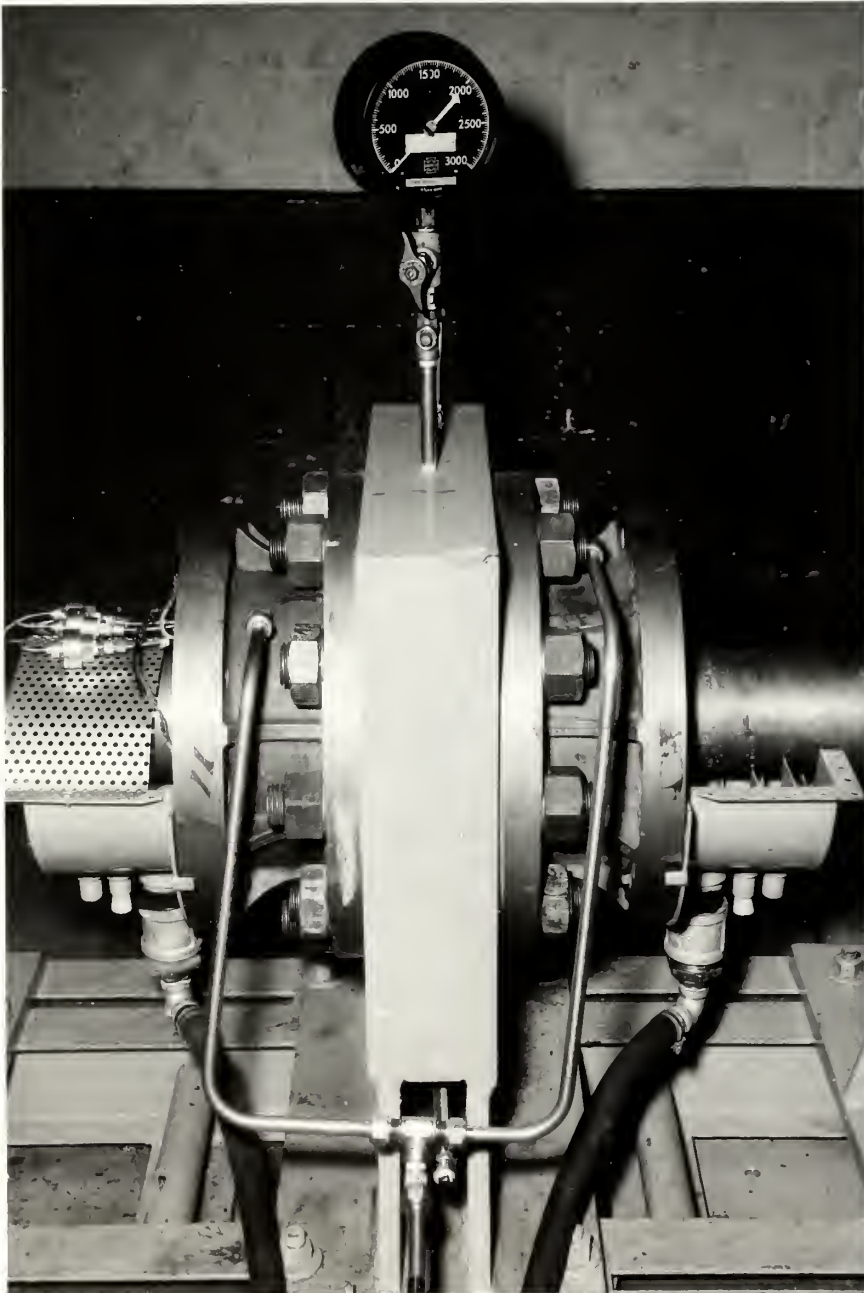


FIGURE VI

TEST SEAL AND CONTROL SEAL INSTALLED IN HOUSING



and torque data was already available from previous testing,⁽⁷⁾ was inserted in the back half of the test rig. Instrumentation was set up to measure the five (5) pressure taps, nineteen (19) thermocouple temperatures, torque, and rpm. (see Figure VII) Filtered river water (brackish) was utilized as the working fluid. Data was taken with the following fixed variables:

| <u>P</u> | <u>N</u> | <u>Q_b</u> |
|----------|----------|----------------------|
| 200 psi | 50 rpm | 0.0 gpm |
| 300 " | 150 " | 0.1 " |
| 500 " | 250 " | 1.0 " |
| 1000 " | 375 " | |
| 1500 " | | |
| 2000 " | | |

Besides the instrumented measurements, inlet pressure, inlet water temperature, seal leakage flow, and seal leakage flow temperature were measured and recorded.

Upon completion of all data taking, the seal ring face was again profiled at the same locations. The results of these profiles (before and after) are shown in Figure VIII.

FIGURE VII
INSTRUMENTATION AND TEST RIG

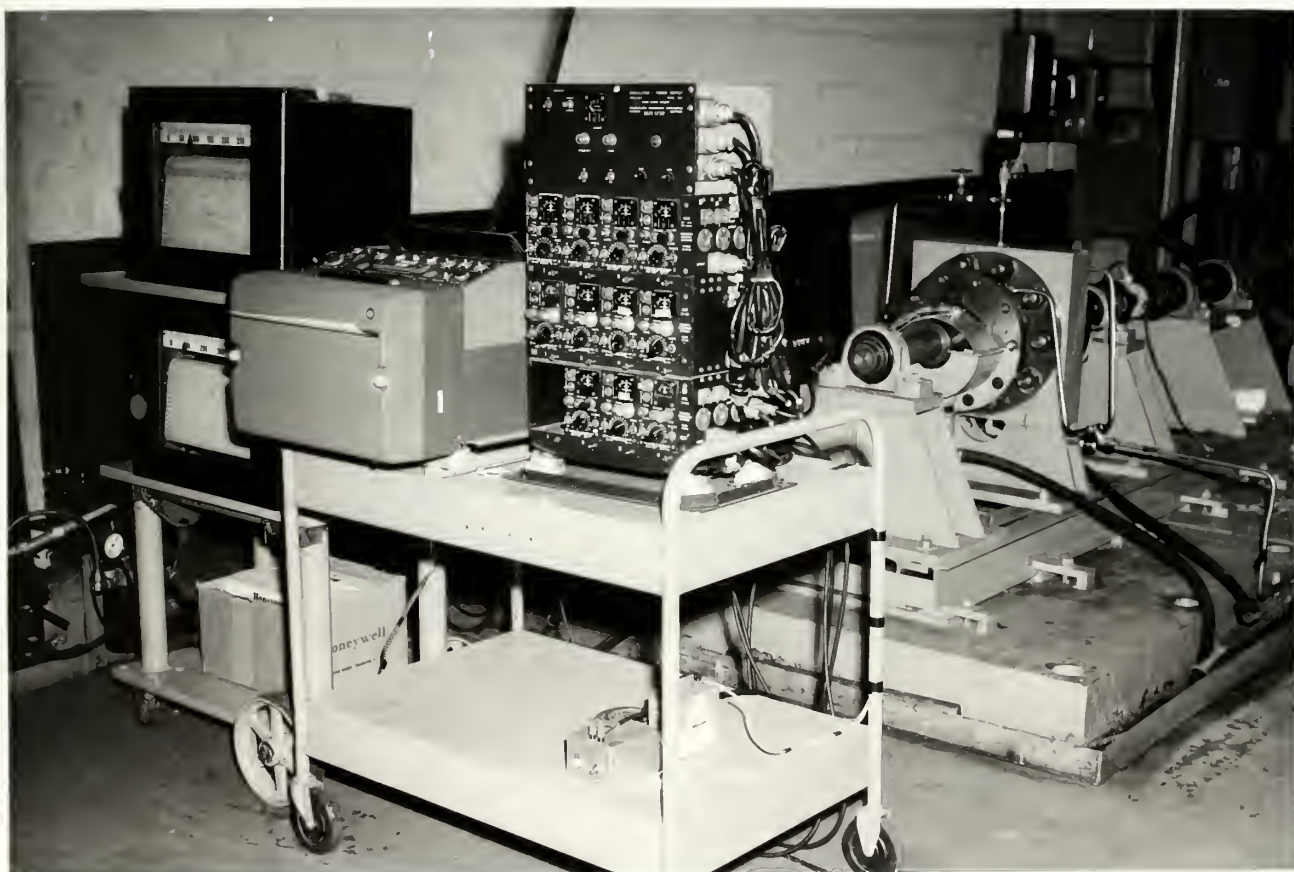


FIGURE VIII

SEAL FACE PROFILES

HIGH
PRESSURE
SIDE

LOW
PRESSURE
SIDE

plotter
error

0.025 inch

0.0002 inch

--Plots spaced
120° apart--

— before test
--- after test

ALI 5/66

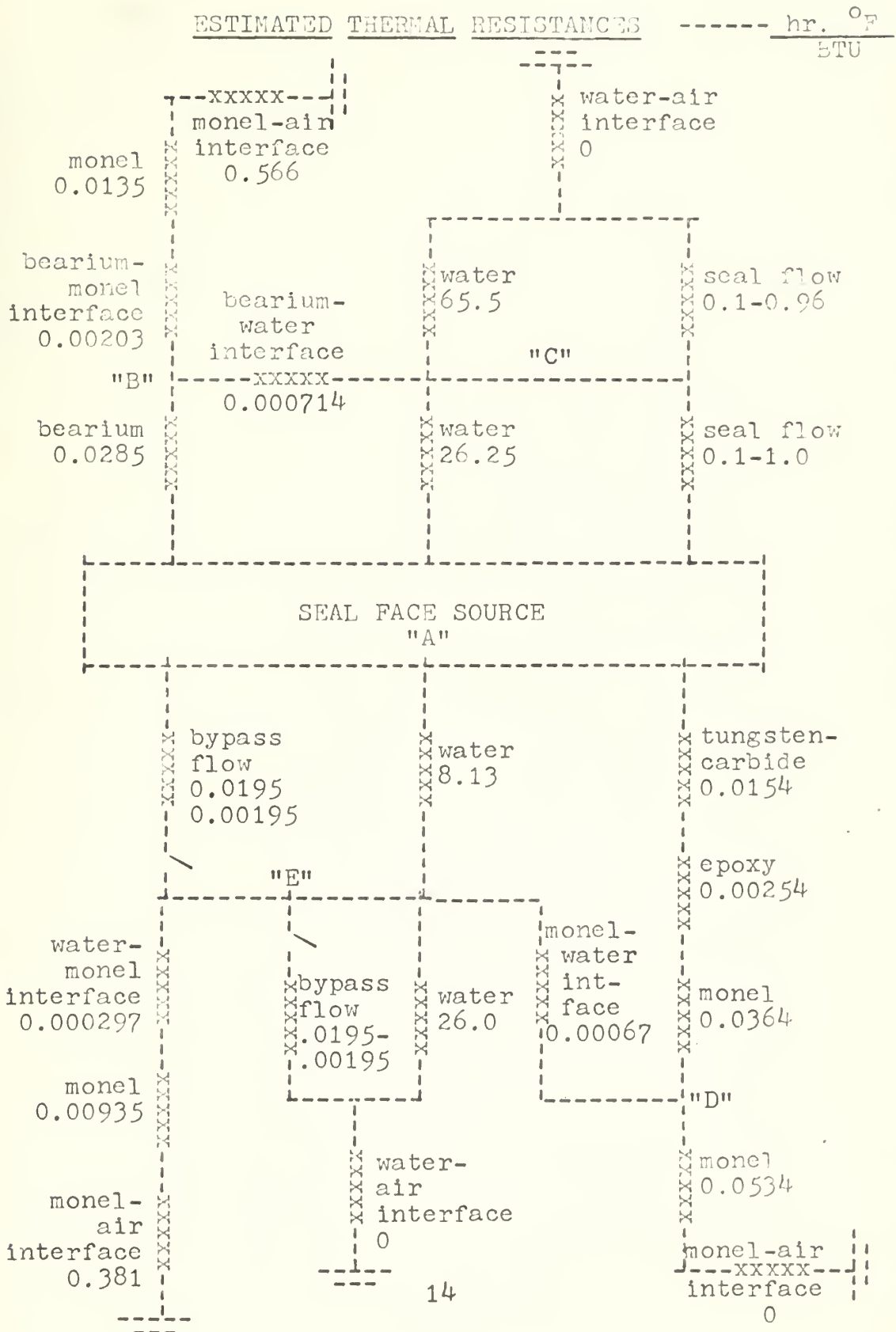
III

ANALYTICAL PROCEDURE

Before determining the quantity of heat generated at the seal interface and the various parameters which are involved in that operation, it was first deemed appropriate to try to set up an analytical model of the seal apparatus. Various techniques were considered and it was finally decided that a lumped model based on thermal resistances and a gross heat source was best suited for this investigation. Thermal resistances were carefully determined based on the most accurate predictions of heat coefficients available and on judicious estimation of the areas and linear distances of the relatively complicated seal geometry.⁽⁸⁾ The convection quantities were determined by the experimentally fixed bypass flow and measured seal leakage flow. (see Appendix A) The final model as utilized throughout the analysis is displayed in Figure IX.

The overall heat input at the seal face is a combination of a variety of heat source components which vary in magnitude with the physical parameters. Basically, there are three calculable contributors to the total heat generation.⁽³⁾ These are the heat generated by the dissipation of pressure energy, the heat generated by viscous shear, and the heat associated with boundary lubrication. Thus

FIGURE IX



the total heat generated at the sealing interface can be calculated from the following equation:

$$q = q_{\text{press}} + q_{\text{visc}} + q_{\text{bound}} \quad (1)$$

or,

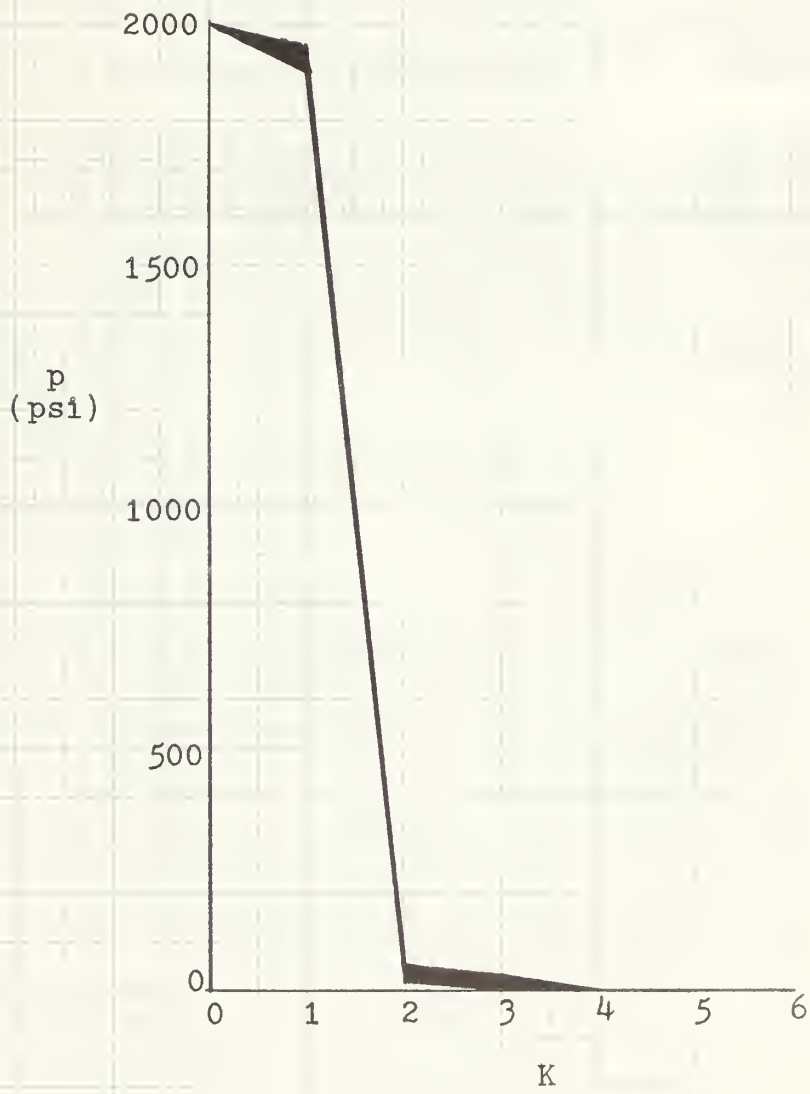
$$q = \frac{Q_f \Delta p}{J} + \frac{\mu A U^2}{J c} + \frac{f A C_p U \Delta p}{J} \quad (2)$$

In the above equation, only the quantity of flow through the sealing faces " Q_f " is an experimentally measured quantity. Pressure drop " Δp " and rotational speed " U " are fixed variables, while face area " A " is fixed by geometric considerations and " μ " and " J " are constant terms. Therefore, those variables remaining to be determined are the coefficient estimating the net average contact stress " C_p ", the seal face clearance " c ", and the coefficient of friction " f ".

The coefficient estimating the net average contact stress " C_p " can be calculated by utilizing the results obtained from the five (5) pressure taps installed in the seal face. The pressure ranges recorded at the five taps spaced at radially equal distances apart are plotted in Figures X, XI, XII, XIII, XIV, and XV. The range of pressures measured for various running conditions of " N " and " Q_b " is plotted against a non-dimensional constant " K ", where " K " is the ratio

FIGURE X

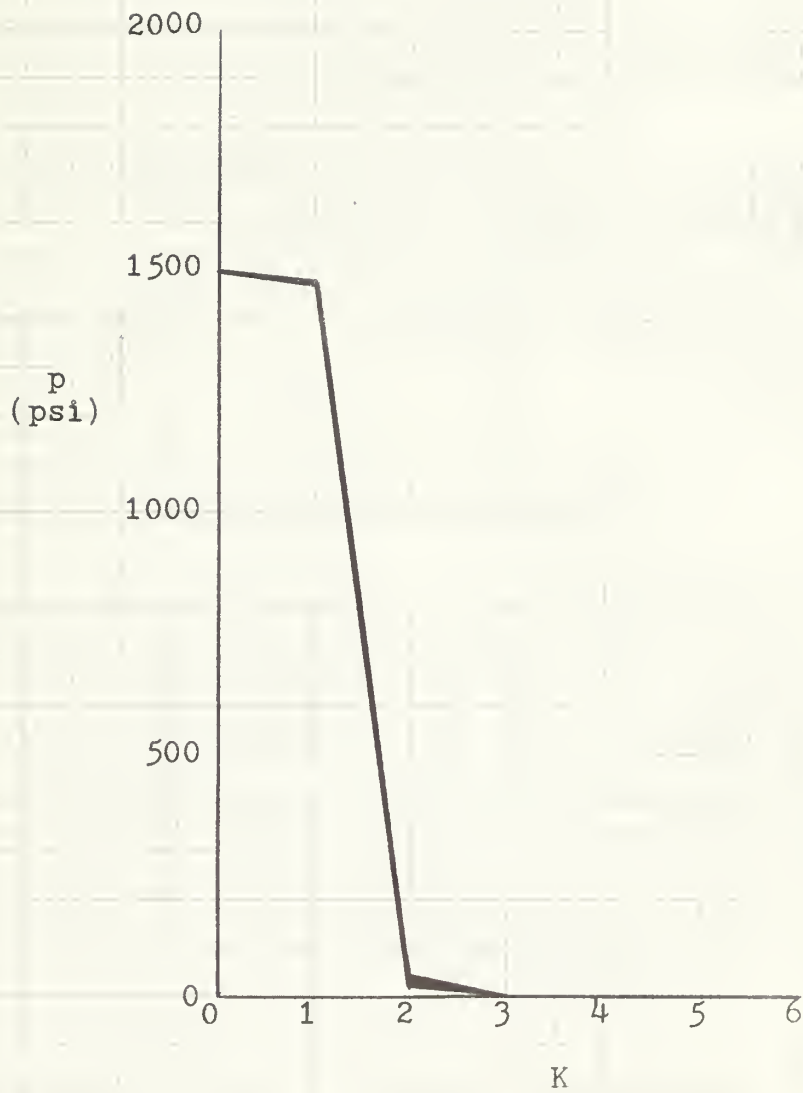
PRESSURE PROFILE RANGE



ALI 5/66

FIGURE XI

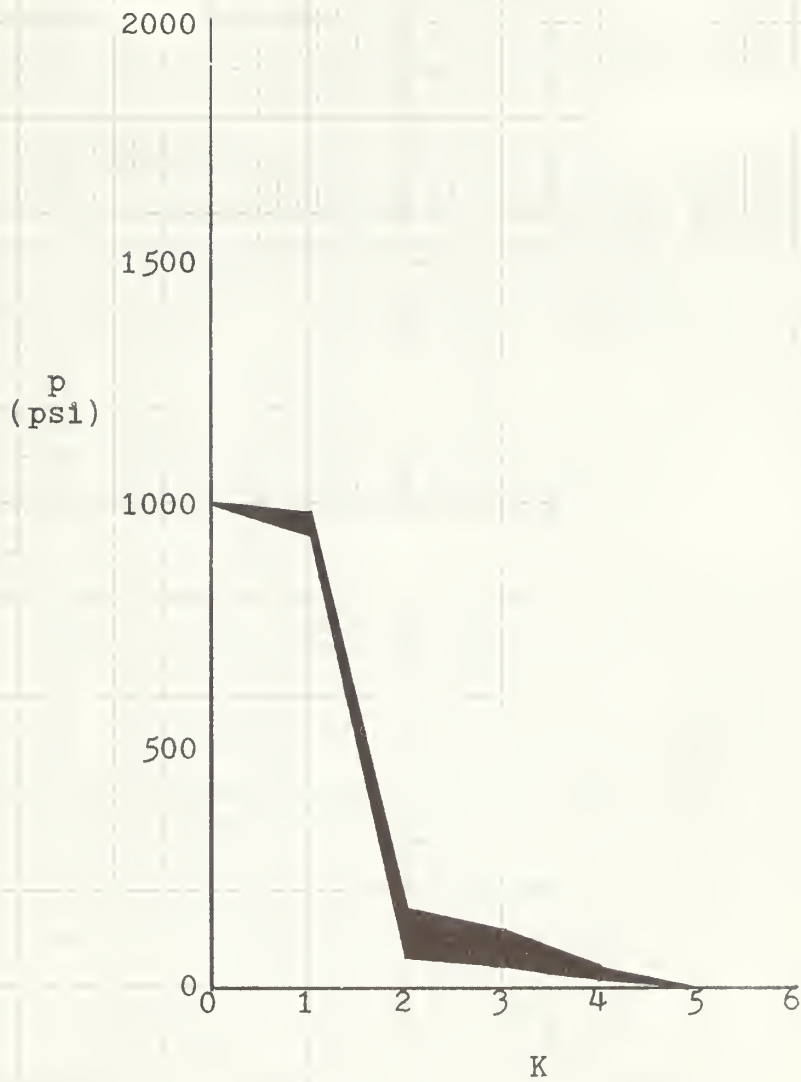
PRESSURE PROFILE RANGE



ALI 5/66

FIGURE XII

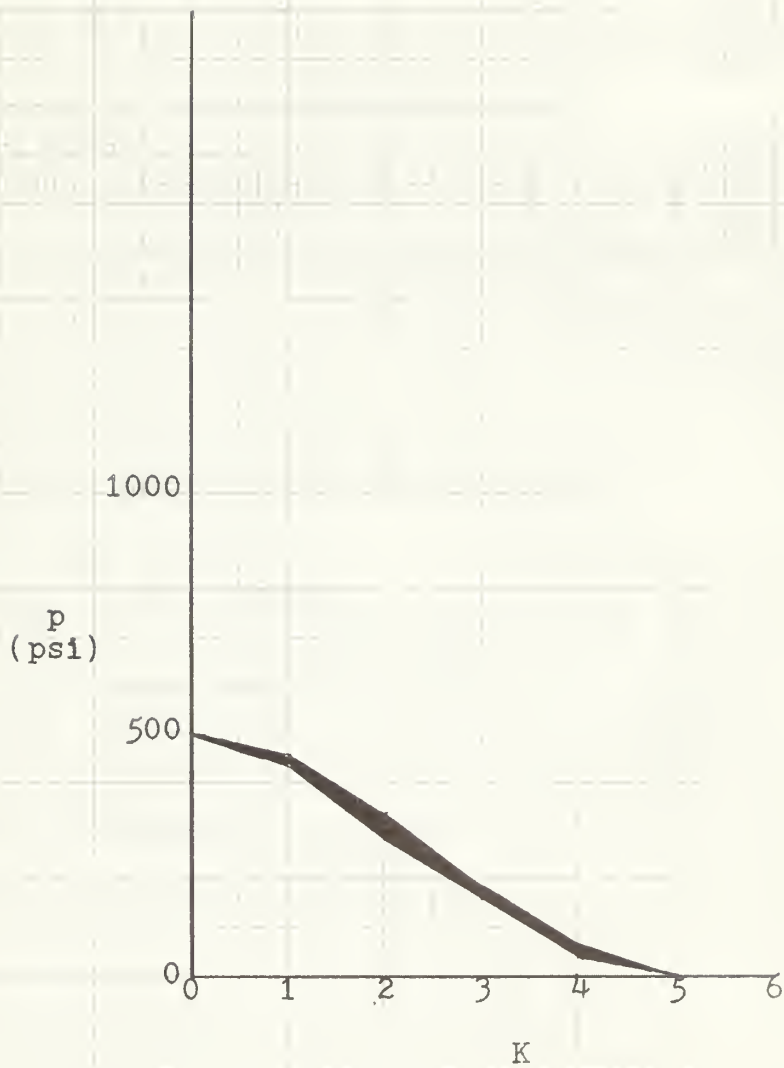
PRESSURE PROFILE RANGE



ALI 5/66

FIGURE XIII

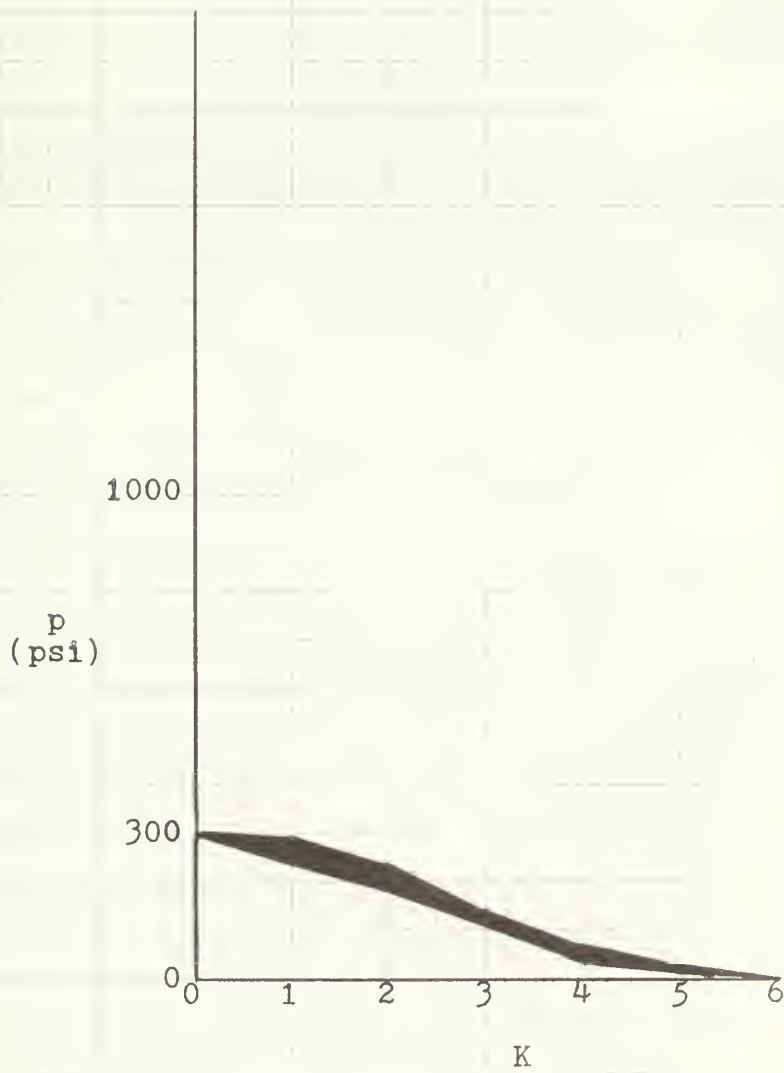
PRESSURE PROFILE RANGE



ALI 5/66

FIGURE XIV

PRESSURE PROFILE RANGE



ALI 5/66

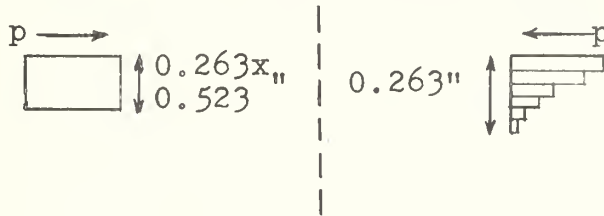
FIGURE XV

PRESSURE PROFILE RANGE



ALI 5/66

of the difference in radii of the outer seal face and the pressure tap to the radial distance between pressure taps. Now, since " C_p " is a function of " p ", and the pressure profiles are known, the seal unbalance may be pictured as:



$$C_p = \frac{\text{closing pressure} - \text{opening pressure}}{\text{inlet pressure}} \quad (3)$$

For example, at " $p = 2000 \text{ psi}$ ", (see Figure X):

$$C_p = \frac{0.523p - (p/6) (0.96+0.05+ 0.02+0.01)}{p} \quad (4)$$

$$= 0.523 - 0.249 = 0.274$$

The balance pressure thus determined and the seal face leakage flow are shown plotted against inlet pressure in Figure XVI.

The seal face clearance " c " for viscous radial flow with " c " and " w " constant can be determined by summing the pressure and shear forces across the fluid film and applying Newton's Law of viscous flow. In simple form:

$$\frac{\Delta p}{w} - \frac{\mu d^2 u}{dy^2} = 0 \quad (5)$$

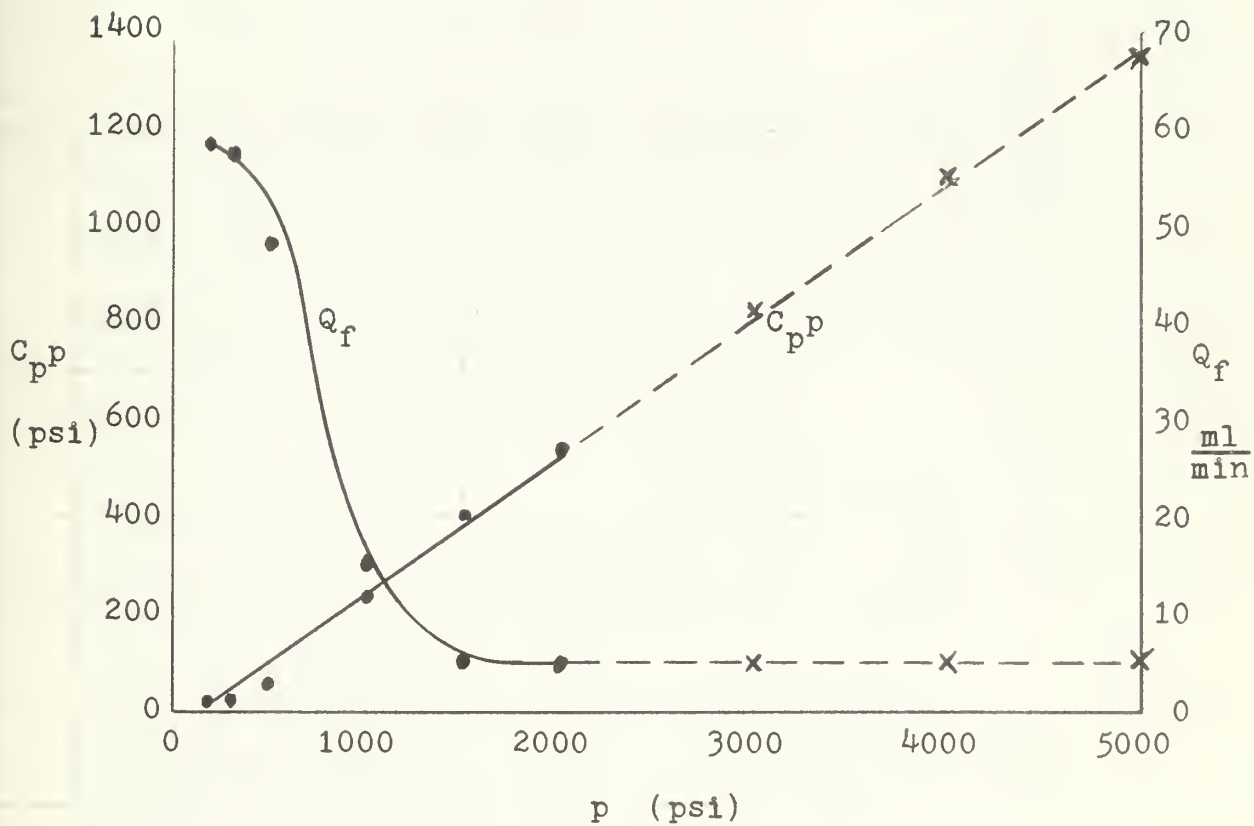
Since the velocity " u " is equal to zero at " $y=0$ " and " $y=c$ ",

FIGURE XVI

BALANCE PRESSURE VS. PRESSURE

and

SEAL FACE FLOW VS. PRESSURE



ALI 5/66

$$u = \frac{1}{2\mu} \frac{\Delta p}{w} (y^2 - cy) \quad (6)$$

Finally, since

$$Q_f = 2\pi R \int_0^c u \, dy, \quad (7)$$

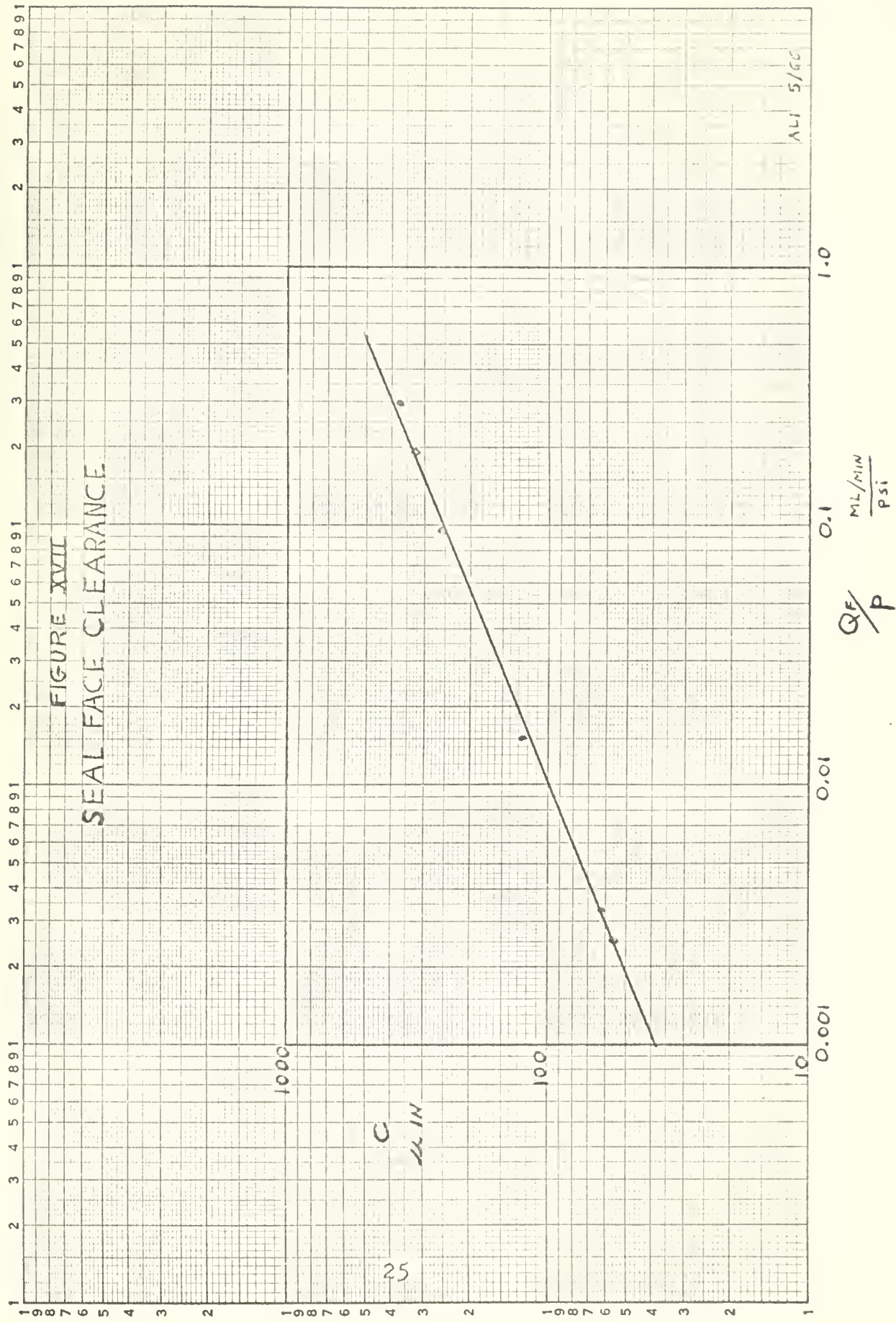
$$Q_f = \frac{\pi R c^3 \Delta p}{6\mu w}. \quad (8)$$

In equation (8), "c" was determined by using a weighing function on "w", based on the percent of seal face actually experiencing the opening pressure. This weighing function was determined from the pressure profiles of Figures X thru XV. For "p = 1000 psi", "2/3 w" was assumed; for "p = 200, 300, and 500 psi", "5/6 w" was assumed; and for "p = 1500 and 2000 psi", "1/3 w" was assumed. Seal face clearance is shown graphically in Figure XVII.

The determination of a reasonable coefficient of friction "f" was finally resolved in the following manner:

$$f = \frac{t}{WR} = \frac{t \text{ (in-lb)}}{20.2 C_p p \text{ (psi)}} \quad (9)$$

Torque data was available from two sources. Original experiment produced some data, but difficulty with the mechanics of the rubber coupling at which the torque-meter was



attached made the results somewhat dubious. Data from similar tests by K. S. Sastelli⁽⁷⁾ provided the author with another source of plotted torque evidence. Both of these sources were weighed and the combined most accurate prediction of torque was determined. The coefficients of friction thus calculated are shown plotted in Figure XVIII against a duty parameter "G" where

$$G = \frac{\mu U W}{W} = 1.224 \times 10^{-9} \frac{N \text{ (rpm)}}{C_p p \text{ (psi)}} \quad (10)$$

With all the variables now accounted for, the total heat input at the seal face source was calculated for all combinations of the fixed parameters:

$$\begin{aligned} p &= 200 - 2000 \text{ psi} \\ N &= 150 - 375 \text{ rpm} \\ Q_b &= 0.0 - 1.0 \text{ gpm} \end{aligned}$$

From Figures XVI, XVII, and XVIII, the variables were extrapolated to include pressures of 3000, 4000, and 5000 psi in order to display the effect of very deep submergence on the heat input and interfacial temperatures. Total heat input, determined as described on the previous pages, is shown graphically as a function of inlet pressure and shaft speed in Figure XIX.

With the heat input as source, and Figure IX as model, an IBM 7094 computer was utilized to determine the nodal temperatures of the resulting 5x5 matrices. (see Appendix B)

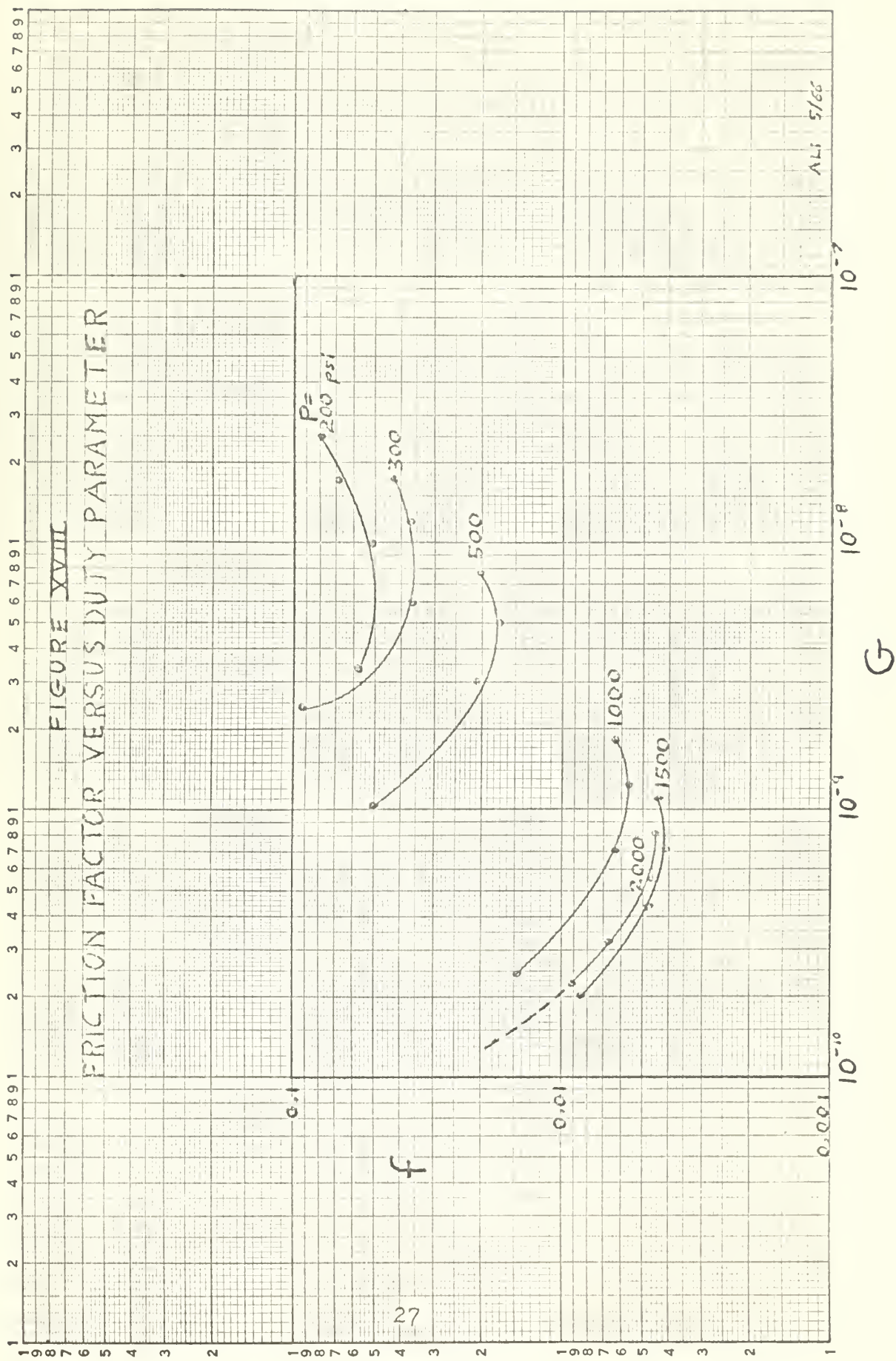
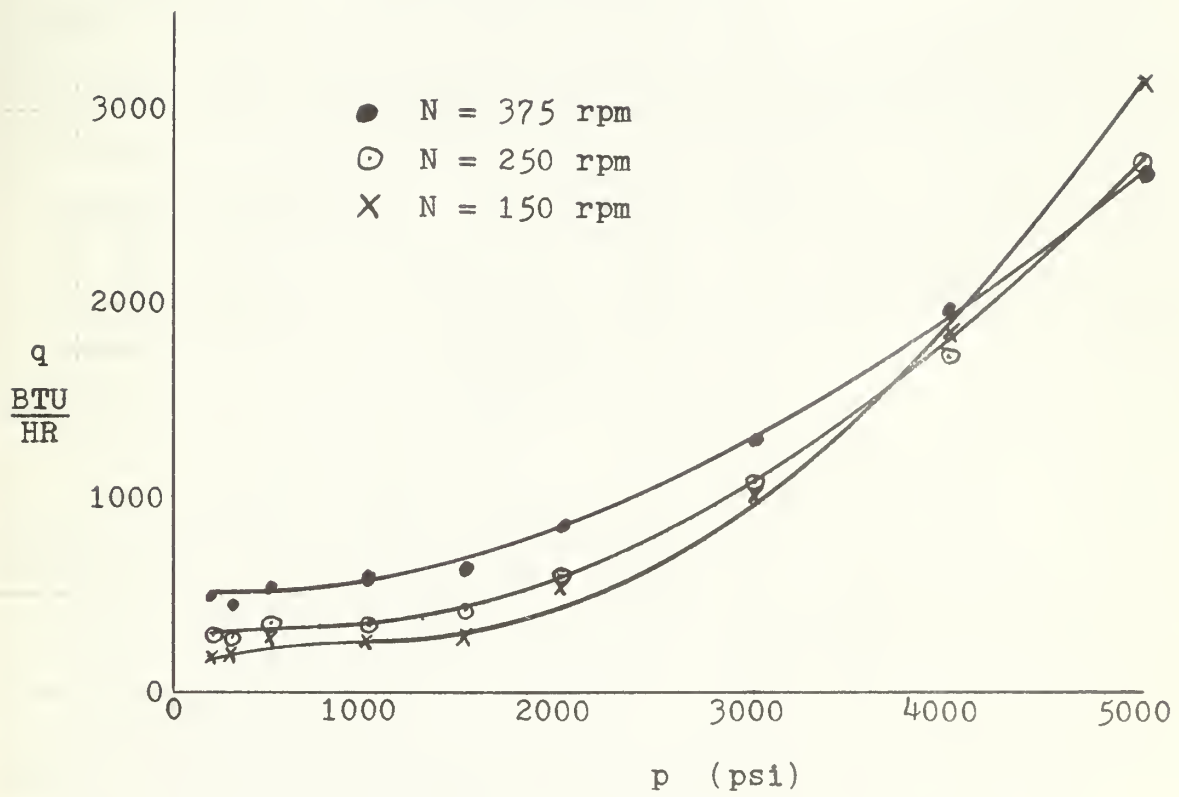


FIGURE XIX

HEAT INPUT VS. PRESSURE



ALI 5/66

IV

RESULTS

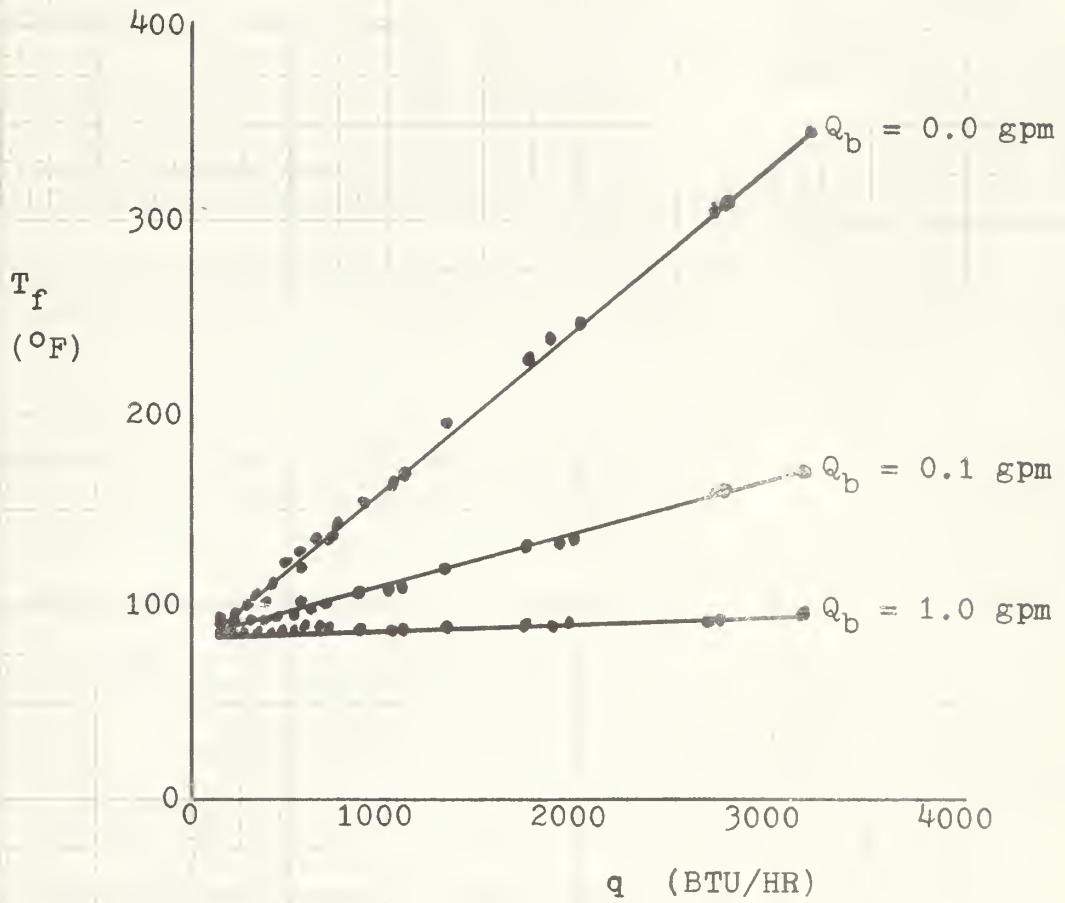
The following thirteen (13) graphs make up the body of thermal experimental and analytical results of this investigation. In Figure XX is shown the actual seal face temperatures (determined analytically) versus the source heat input. Figures XXI and XXII show actual seal face temperature (determined analytically) plotted against inlet pressure for bypass flows of 0.0 and 0.1 gpm respectively. Figures XXIII through XXXII depict both an analytical and an experimental non-dimensional temperature quantity "T", where

$$T = \frac{T_f - T_a}{T_a} \quad . \quad (11)$$

This is plotted against " Q_b ", the bypass flow rate, for varying inlet pressure from 200 to 5000 psi. Note that Figure XXVIII is a duplicate presentation of Figure XXIX with the exception of the scale utilized. Note also that all data in Figures XXX, XXXI, and XXXII is from the analytical extrapolation.

FIGURE XX

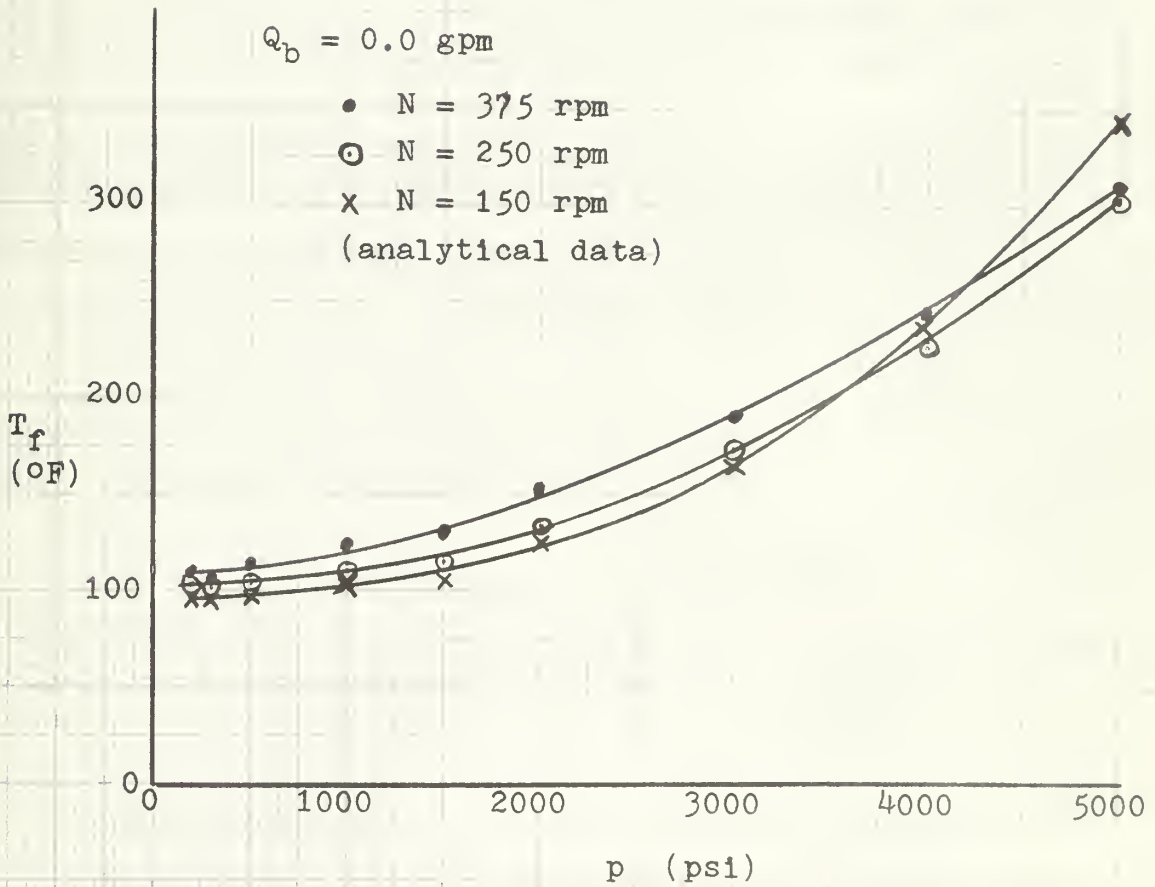
SEAL FACE TEMPERATURE VS. HEAT INPUT



ALI 5/66

FIGURE XXI

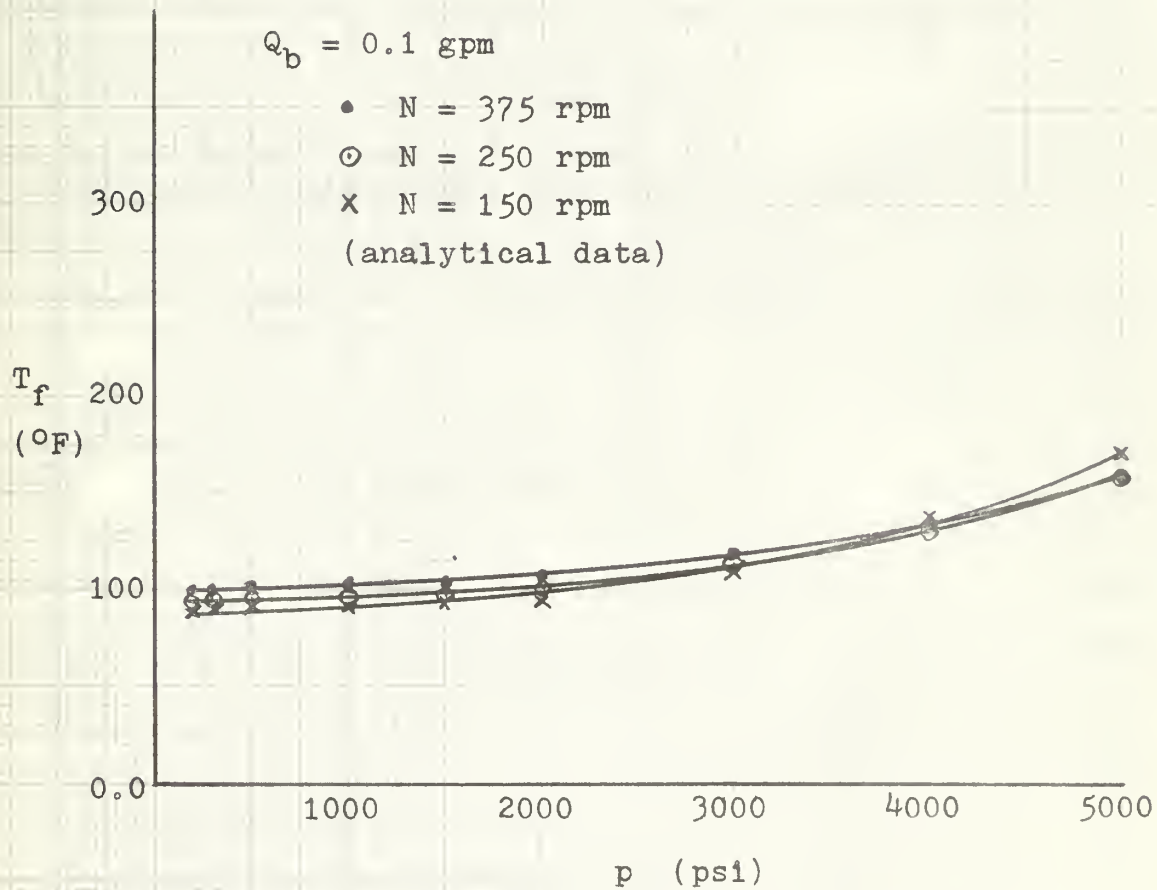
SEAL FACE TEMPERATURE VS. PRESSURE



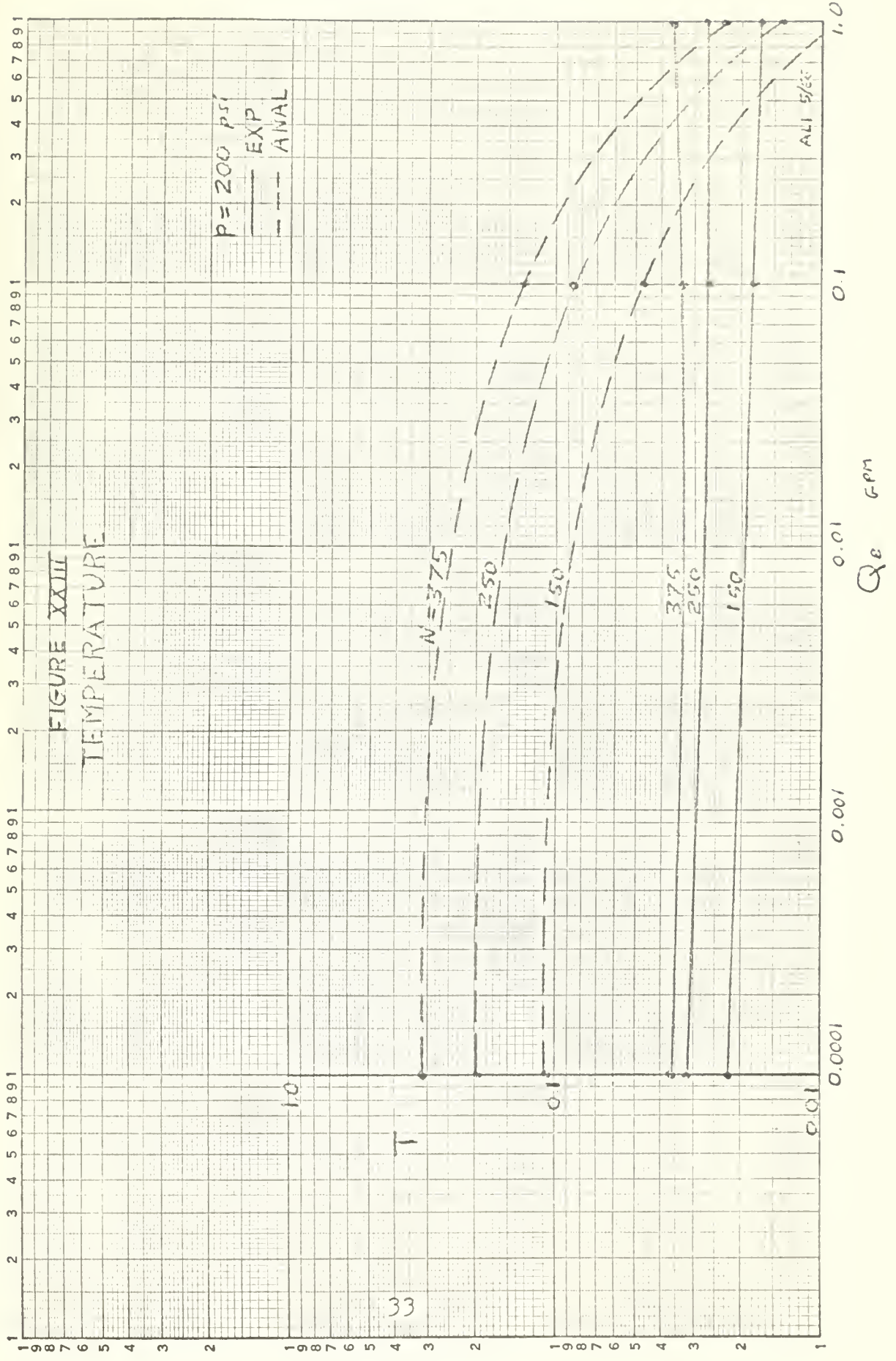
ALI 5/66

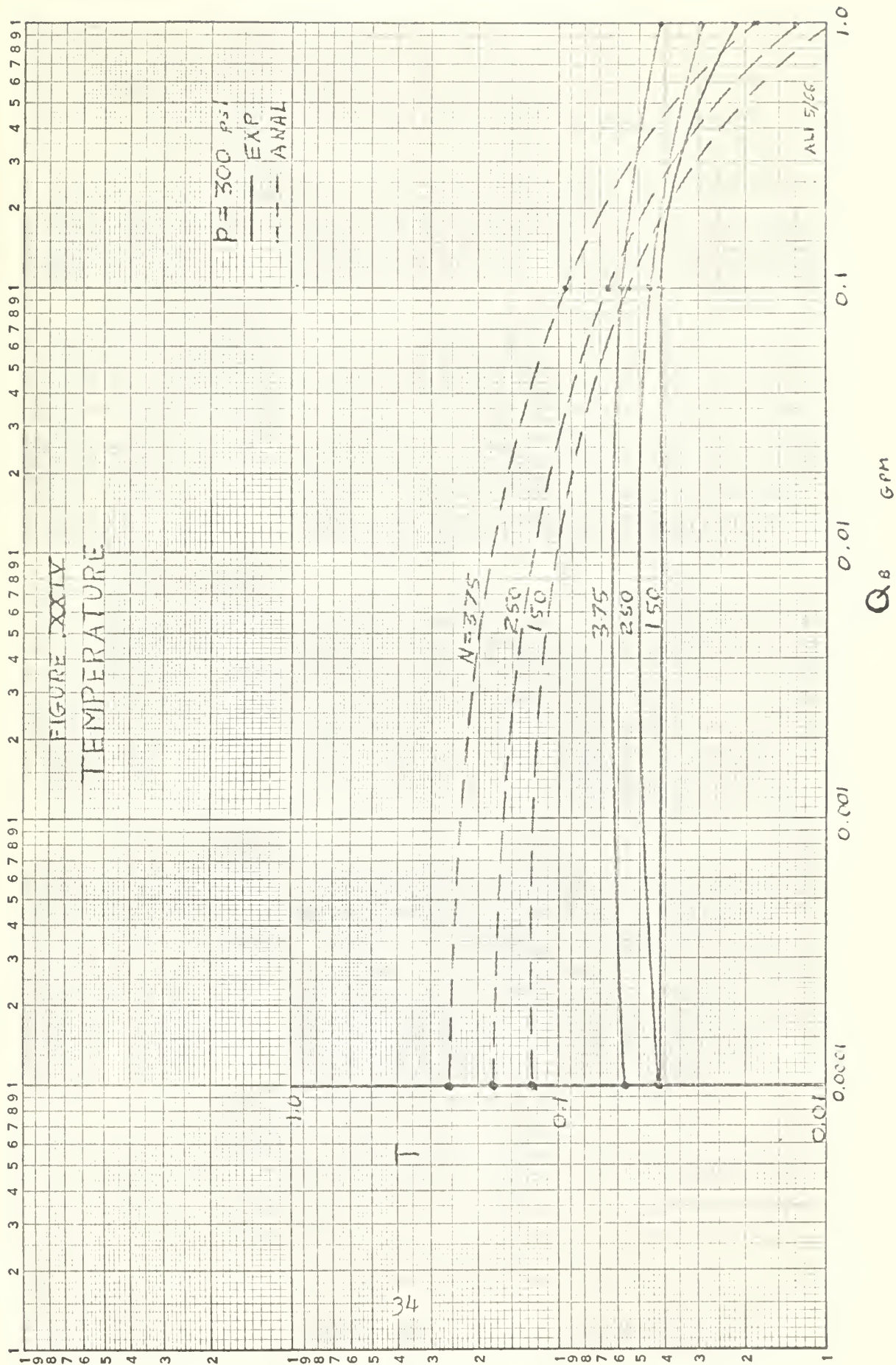
FIGURE XXII

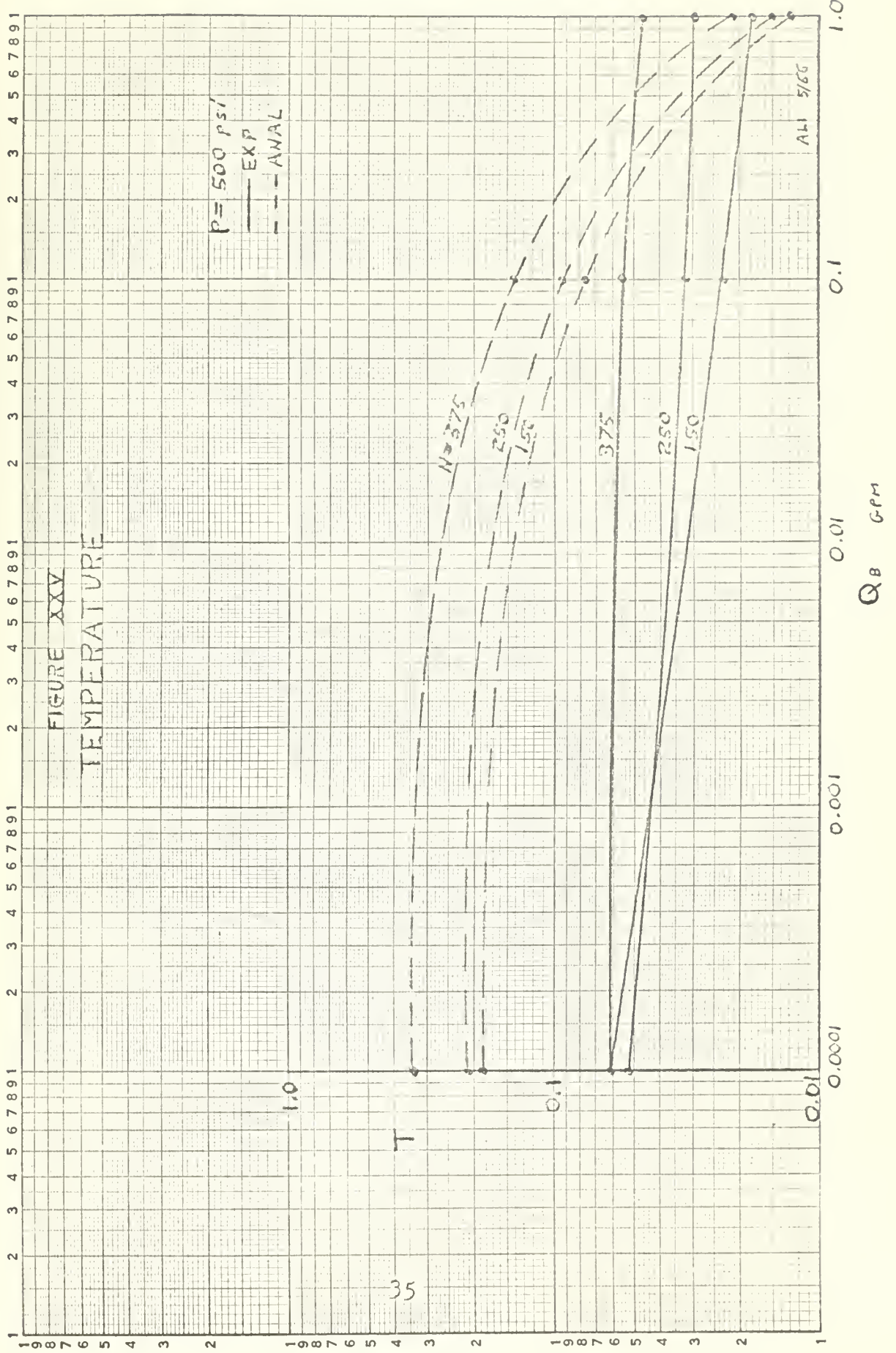
SEAL FACE TEMPERATURE VS. PRESSURE

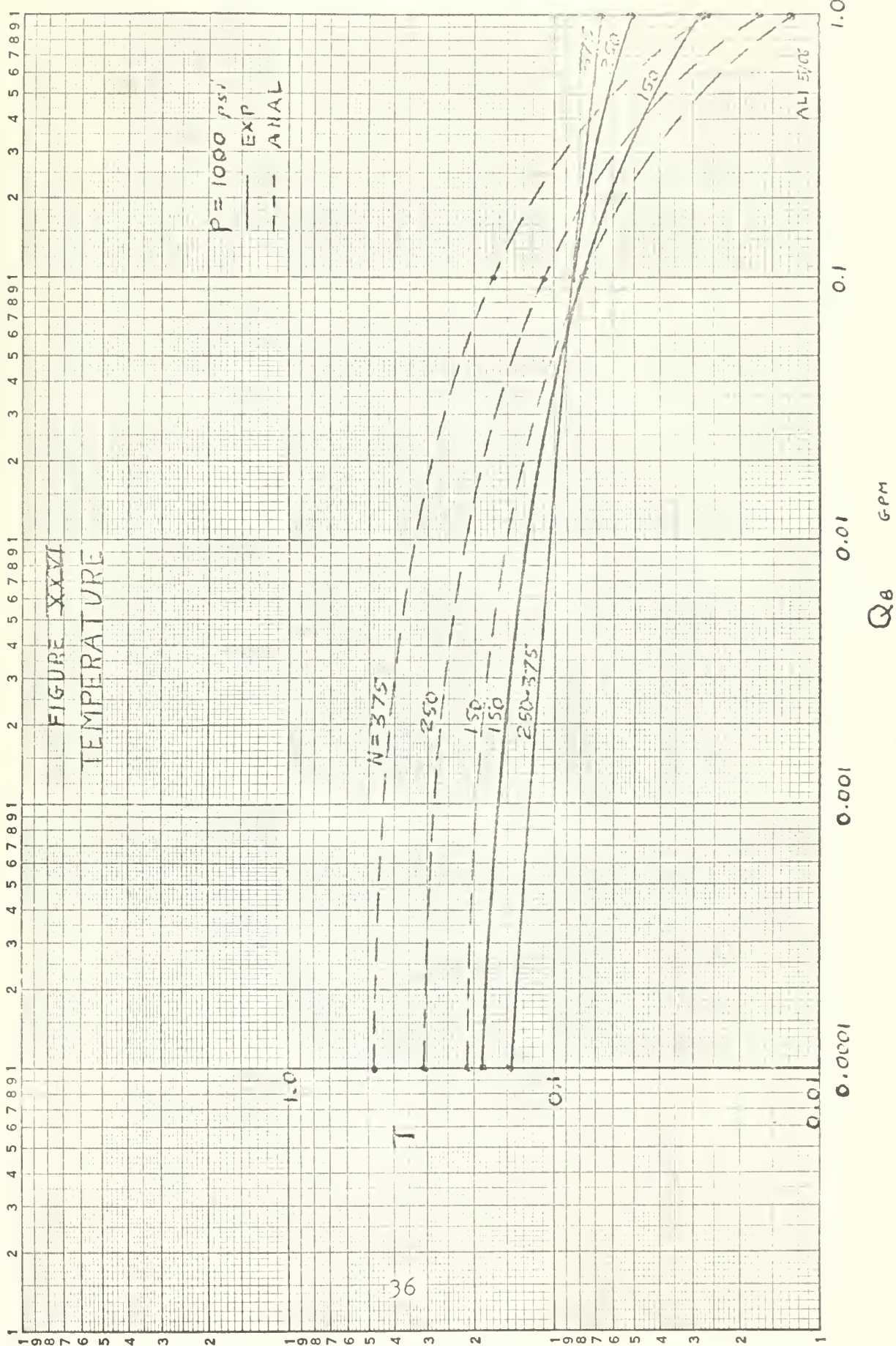


ALI 5/66









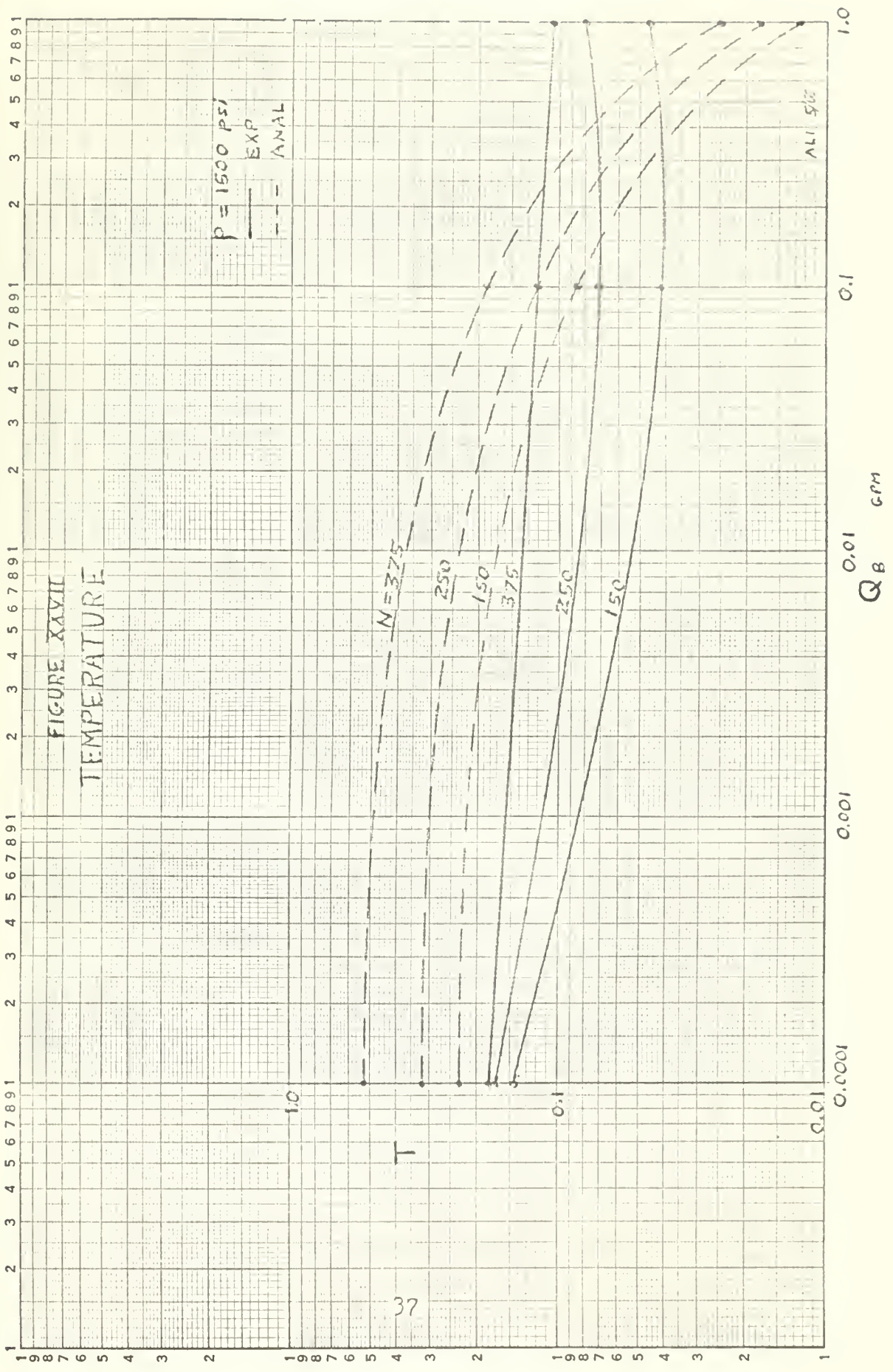
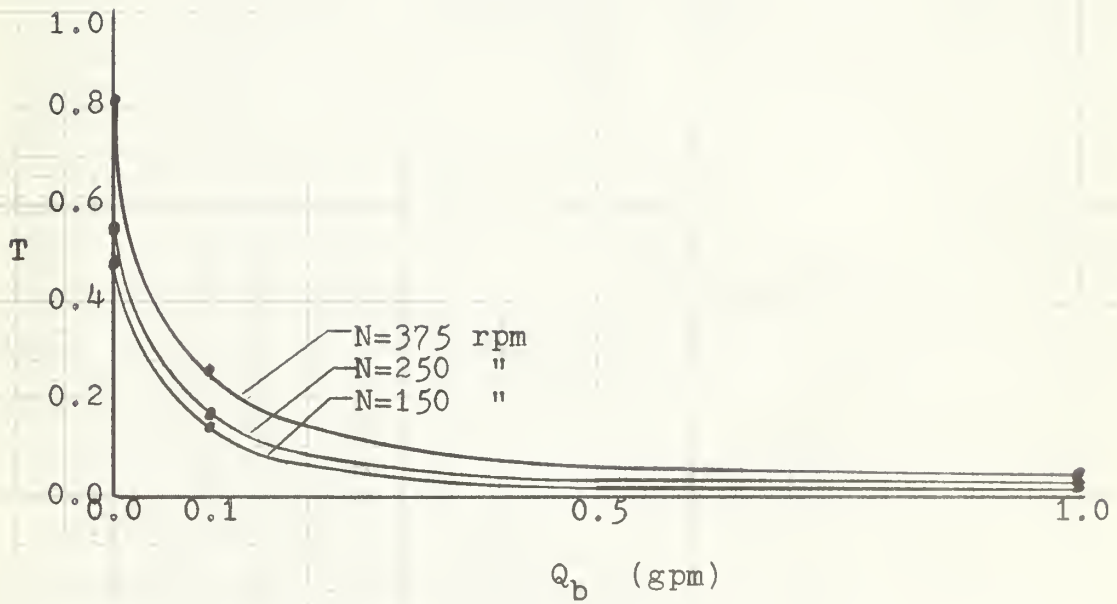


FIGURE XXVIII

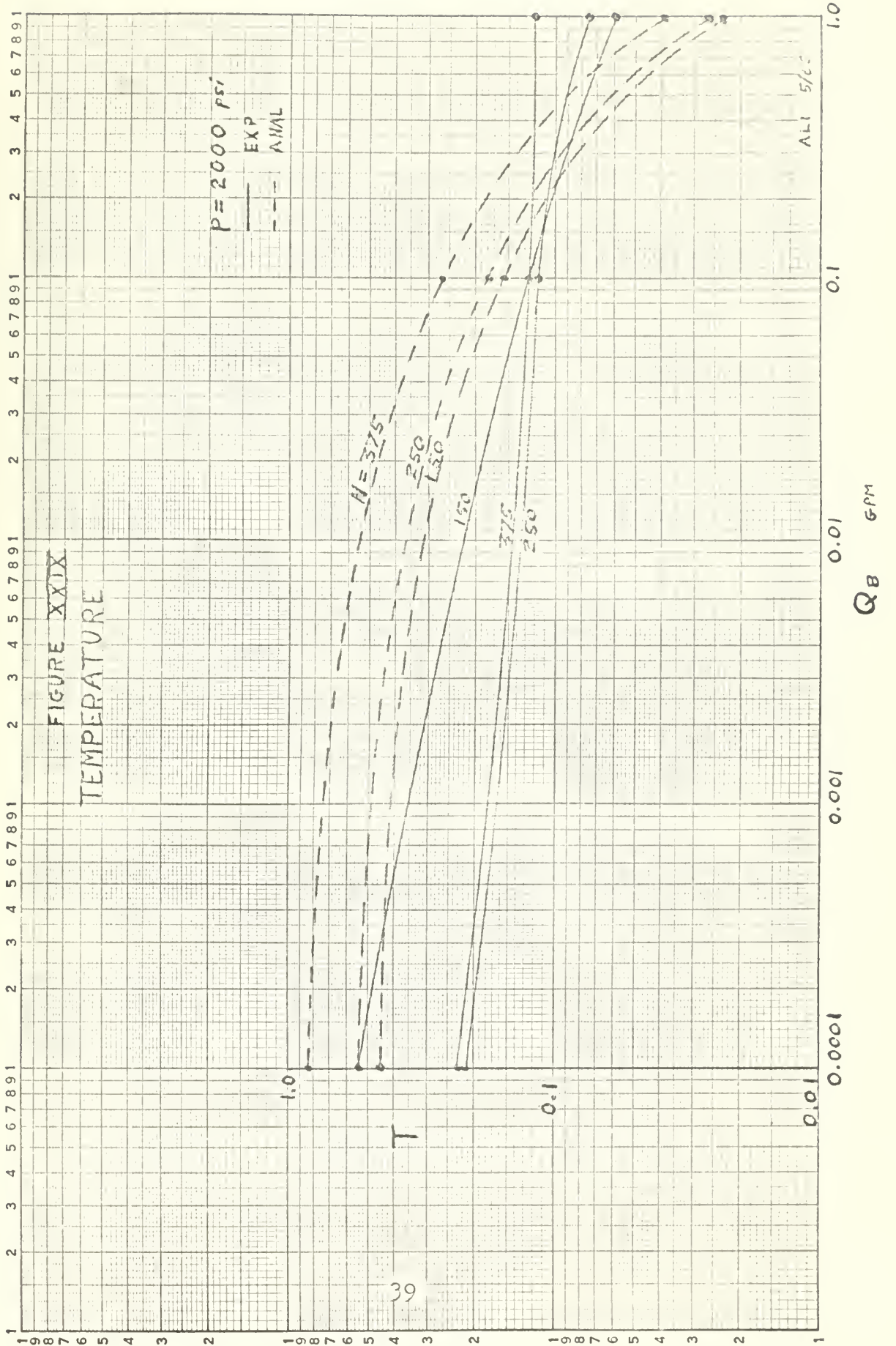
TEMPERATURE

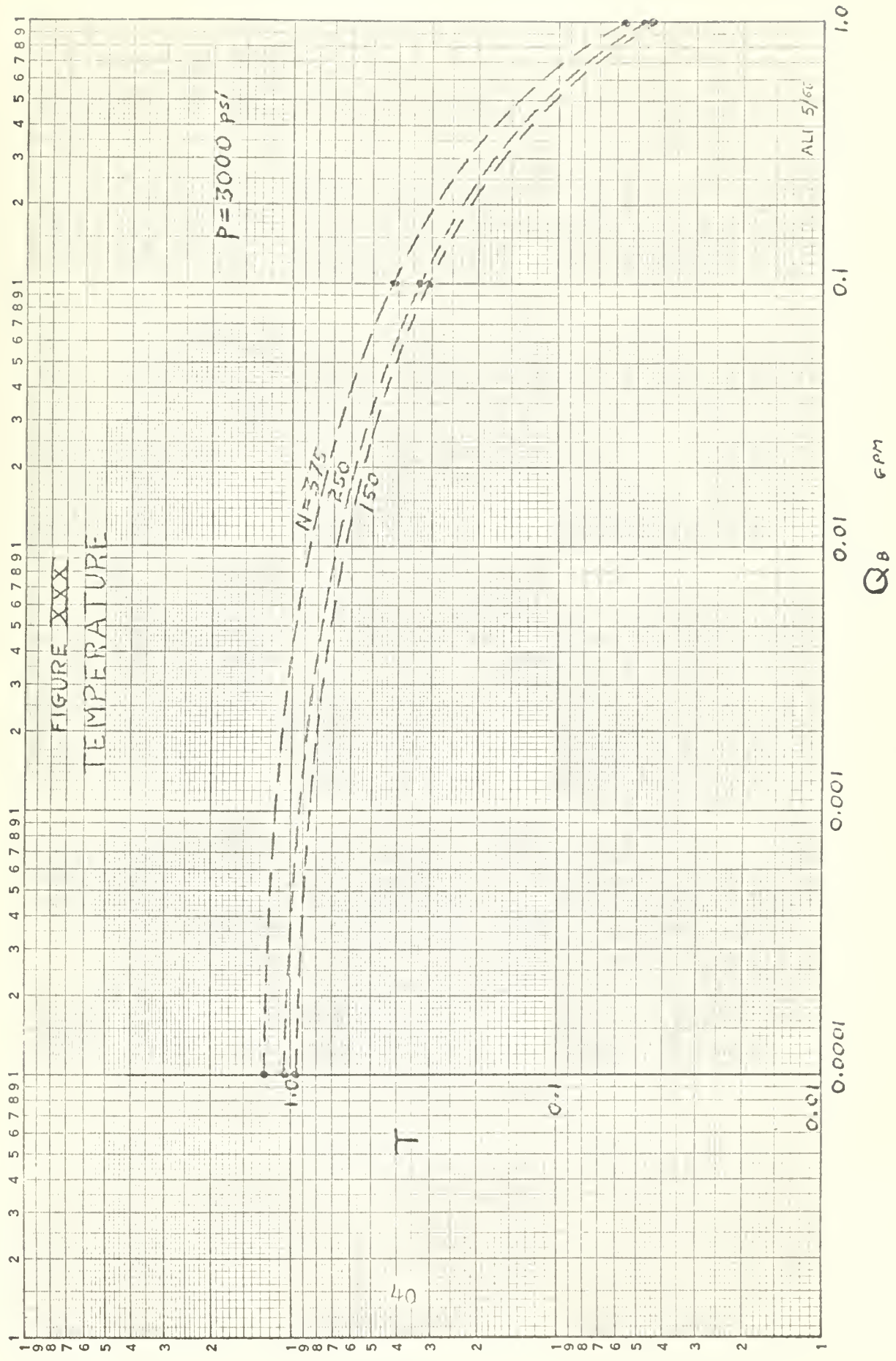
$p = 2000 \text{ psi}$

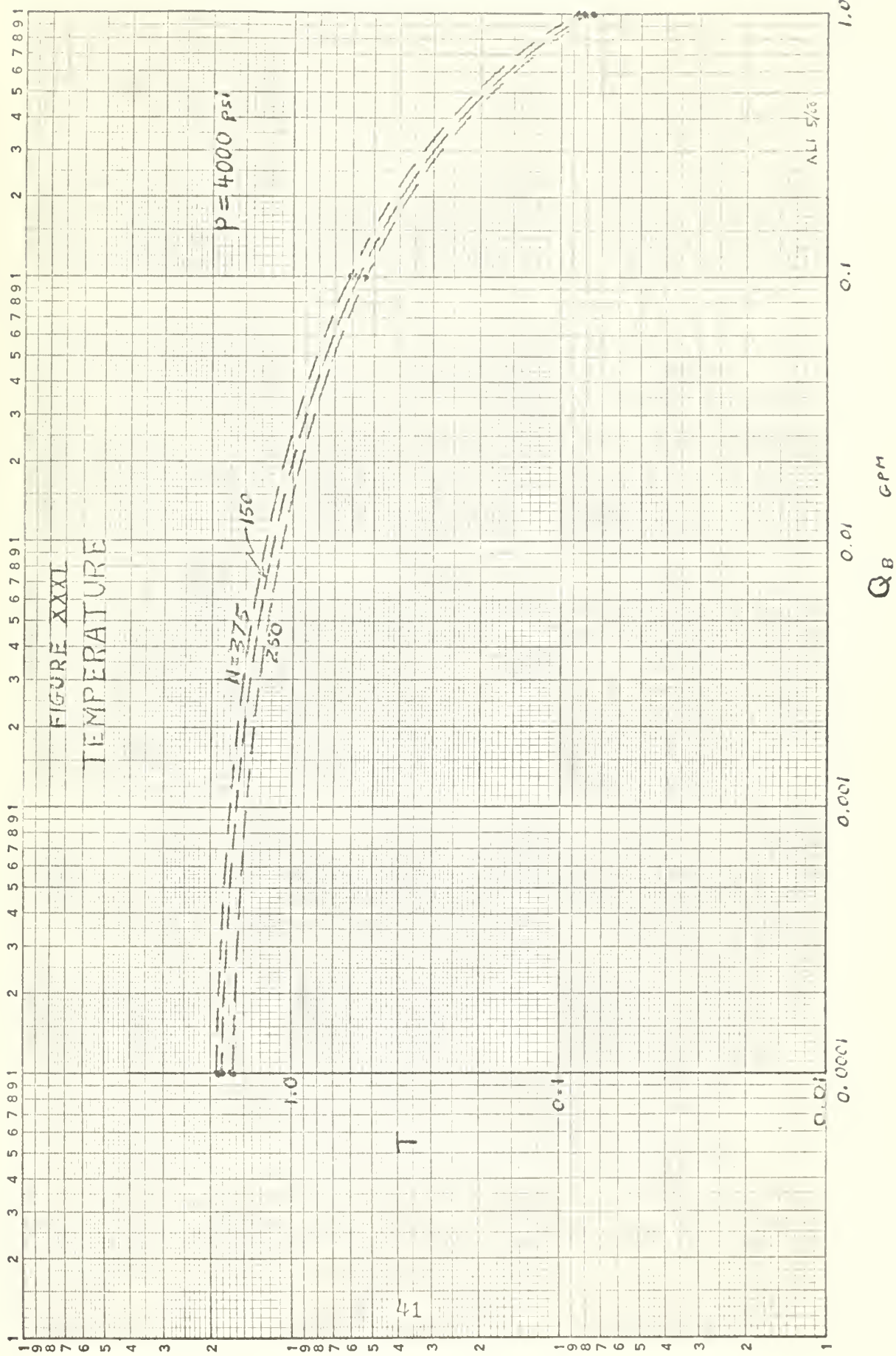
(analytical data)

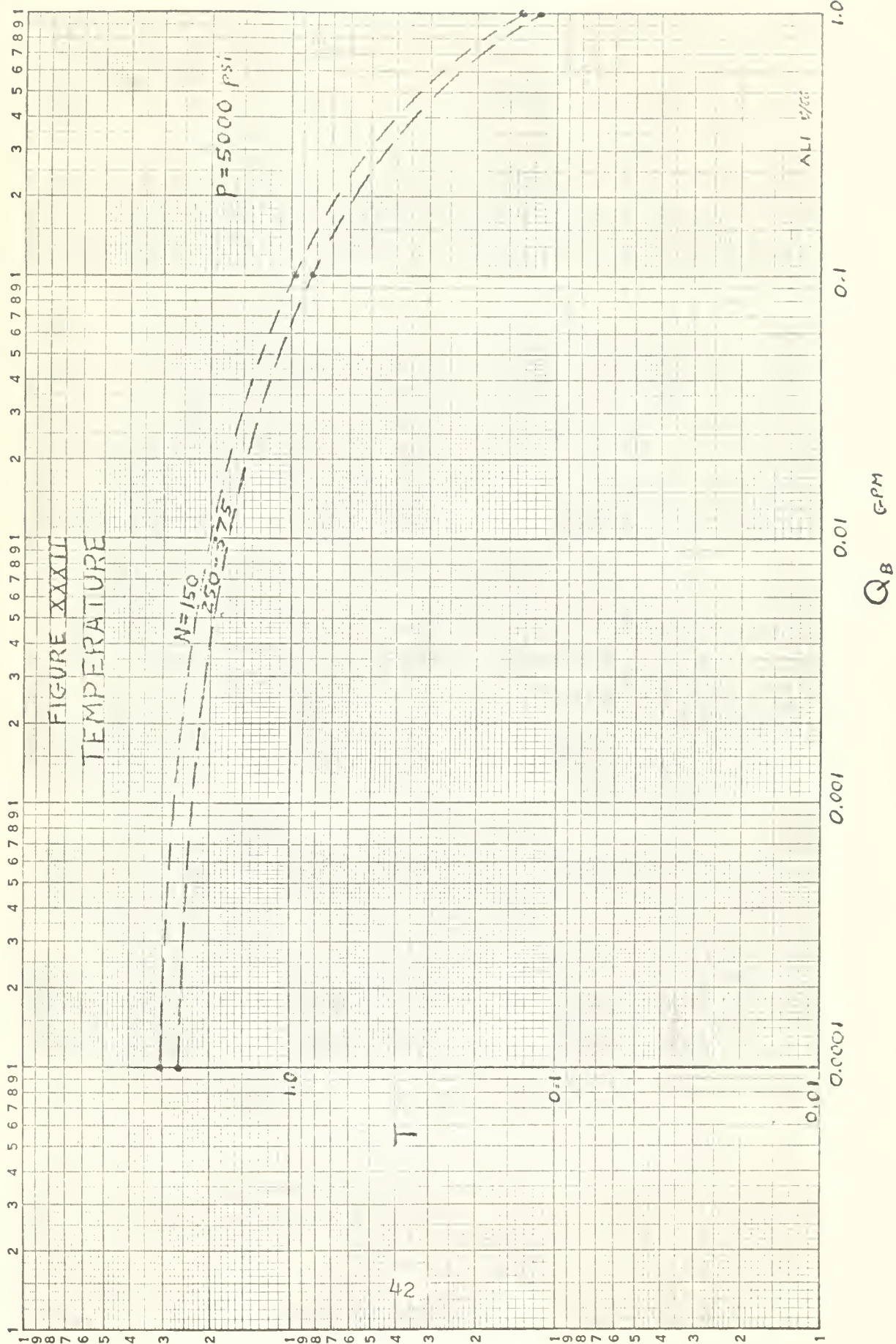


ALI 5/66









V

DISCUSSION OF RESULTS

The first three figures of Chapter IV present, in capsule form, the major points learned from this investigation. The most obvious and also most important result is best seen in Figure XX on page 30. With no bypass cooling water flow, the seal interfacial temperature rises sharply with heat input, so swiftly in fact that a heat input of only about 1600 BTU/HR is required for vaporization of the film. However, it can be seen that only a very slight quantity of bypass cooling water flow (0.1 gpm) will decrease the temperature rise to a safe level for even the highest predicted value of heat input. Further, if the quantity of bypass cooling water flow is increased to 1.0 gpm, the seal interfacial temperature rise is almost negligible for even large increases in heat input.

Figures XXI and XXII on pages 33 and 34 respectively display the same phenomena when examined together. Taken separately, some further discussion presents itself. In Figure XXI, it can be seen that for zero bypass cooling water flow, the limiting seal inlet pressure is between 3400 psi and 3700 psi, depending on the rotational speed of the apparatus. A very interesting phenomenon also discernable in this Figure is the sharper rise in temperature of the low

speed analytical data at high values of input pressure. This can be attributed first to the results of Figure XIX on page 28, which in turn is really a function of the three heat input variable terms. Further examination of the analytical data shows that the key lies in the heat associated with boundary lubrication, the third term in the heat equation (Equation (2) on page 15). For example, the low value of duty parameter " $G=1.34 \times 10^{-10}$ " at " $p=5000\text{psi}$ " and " $N=150\text{rpm}$ " results in a relatively high value of the coefficient of friction " $f=0.018$ ", as can be seen on the extrapolated portion of Figure XVIII on page 27.

The same phenomenon is also discernable (to a lesser extent) in Figure XXII on page 32. Here, with a small amount of bypass cooling water flow, the temperature rises are not very sharp, and are also not significantly dependent on RPM.

At very low pressures, the spread of results between the experimental and the analytical data was a maximum. (see Figures XXIII, XXIV, and XXV) However, at higher values of the seal inlet pressure ($p = 1000\text{ psi}$ and above) the experimental and analytical results show a marked similarity in trends and values. It is extremely interesting to note that the trend for the combination of low RPM and high pressure to result in a greater heat input and hence higher interfacial temperature begins at a considerably lower pressure in the experimental results than it does in the analytical data.

The fact that this trend did exist both experimentally and analytically is quite significant.

The curves of Figure XXVIII on page 38 display in true focus the sharp rise in the temperature associated with decreased bypass cooling water flow. It would have been desirable to display all of the temperature increases in this form, but this would have resulted in the curves being so bunched as to be unreadable; hence the logarithmic displays.

VI

CONCLUSIONS AND RECOMMENDATIONS

Deep submergence submarine shaft seals of a similar design to those presently being used require a minimum amount of bypass cooling water flow. Any design change that would limit or eliminate the source of cooling water must be carefully evaluated as to the thermal implications involved. It is recommended that the method of evaluation should follow that presented in the Analytical Procedure and in the Appendices of this paper.

Further, in any investigation of this type, due consideration should be given the low-speed/high-pressure limiting condition. This warning is especially emphasized since one would intuitively expect that a high-speed/high-pressure limiting condition would be all that required examination.

In future experimental investigations with submarine shaft seals, it is recommended that a more satisfactory method of gathering accurate torque data be devised and utilized. Only then can a great deal of confidence be given the computed coefficients of friction and hence heat source inputs.

Finally, computer programs similar to that described in Appendix B are available in most large computation centers, and ought to be utilized in investigations of this nature.

APPENDIX

APPENDIX A
DETERMINATION OF THERMAL RESISTANCES

The thermal resistances shown diagrammatically in Figure IX on page 14 were calculated from the following basic equations:

$$q = h A \Delta T \quad ; \quad R = \frac{1}{h A} \quad (12)$$

$$q = \frac{k A \Delta T}{L} \quad ; \quad R = \frac{L}{k A} \quad (13)$$

$$q = Q C \Delta T \quad ; \quad R = \frac{1}{Q C} \quad (14)$$

The following constant coefficients were established:

| | $\frac{k}{\text{hr ft } ^\circ\text{F}}$ | $\frac{h}{\text{hr ft}^2 ^\circ\text{F}}$ | $\frac{C}{\text{lb } ^\circ\text{F}}$ |
|-------------------------|--|---|---------------------------------------|
| Bearium | 20.4 | | |
| Monel | 15.0 | | |
| Tung. Carb. | 30.0 | | |
| Epoxy | 0.6933 | | |
| Cooling Water | 0.33 | | 1.0 |
| Monel-air Interface | | 0.8 | |
| Bearium-Monel Interface | | 1000.0 | |
| Monel-Water Interface | | 3570.0 | |
| Bearium-Water Interface | | 5950.0 | |

The value of " Q_b " was set either at 0.0 (closed circuit) or at 0.1 or 1.0 gpm. Values of " Q_f " were determined individually for the range of pressures utilized. (see Figure XVI on page 23)

The following cross-sectional areas of heat transfer surface and lengths of heat transfer paths were estimated by examination of the particular geometry of the seal under study. A similar analysis would be required for any modification in seal geometry. However, for a simple scaling modification, the areas and linear distances could be similarly scaled.

| | <u>A</u> (in ²) | <u>L</u> (in) |
|--|-----------------------------|---------------|
| Bearium | 31.0 | 1.5 |
| Bearium-Monel Interface | 71.0 | |
| Monel (seal ring housing) | 71.0 | 1.2 |
| Monel-Air Interface (seal ring housing) | 318.0 | |
| Bearium-Water Interface | 34.0 | |
| Sealing Water at Face | 2.1 | 1.4 |
| Sealing Water at Leakoff | 1.0 | 1.8 |
| Seal Water-Air Interface | ∞ | |
| Tungsten Carbide | 13.0 | 0.5 |
| Epoxy | 34.0 | 0.005 |
| Monel (face ring housing) | 22.0 | 1.0 |
| Monel (shaft) | 150.0 | 10.0 |

| | <u>A</u> (in ²) | <u>L</u> (in) |
|--|-----------------------------|---------------|
| Monel-Air Interface (shaft) | ∞ | |
| Monel-Water Interface (face ring housing) | 60.0 | |
| Bypass Water at Face Ring Housing | 7.0 | 1.6 |
| Water-Monel Interface (seal housing) | 157.0 | |
| Monel (seal housing) | 171.0 | 2.0 |
| Monel-Air Interface (seal housing) | 472.0 | |
| Bypass Water at Bypass Channel | 14.0 | 10.0 |
| Bypass Water-Air Interface | ∞ | |

APPENDIX B
COMPUTATIONAL PROCEDURE

The computer program utilized in this thesis can be found in the Department of Naval Architecture and Marine Engineering Computer Library at the Massachusetts Institute of Technology under the coding of NA 021.0. The computer listing follows:

```

      FORTRAN
      DIMENSION A(11,11),B(11,11),X(11),E(11),IL(20)
500  READ 400, JOB
400  FORMAT (I5)
      IF (JOB) 501,502,503
501  CALL EXITM
502  CALL EXIT
503  IF (JOB-2)100,200,300
C     PART 1 SIMULTANEOUS EQUATION SOLN BY XSIMEQF
C F FACTOR BY WHICH XSIMEQF MULT. VALUE OF DET. A(I,J)
C JJ=NUMBER OF COLUMNS IN MATRIX B
C M=1 SOLN GOOD,BRIGHT BOY,A(I,J) REPLACED BY X(I,J)
C M=2 OVERFLOW, BROKE THE BANK
C M=3 MATRIX A IS SINGULAR, GO TO JAIL
100  READ 15
      PRINT 15
      READ 10,N,((A(I,J),I=1,N),J=1,N)
      PRINT 11,N
      DO 16 I=1,N
      PRINT 19,(A(I,J),J=1,N)
16   CONTINUE
      PRINT 24
      READ 2,(B(K,1),K=1,N)
      PRINT 2,(B(K,1),K=1,N)
2    FORMAT (5F13.4)
      PRINT 17
      PRINT 18
      PRINT 24
10   FORMAT (I5/(5F13.4))
11   FORMAT (4H N= ,I3)
12   FORMAT (16H GOOD BOY DET = ,1PE14.6/(op5F14.5))
13   FORMAT (16H BROKE THE BANK)
```



```

14  FORMAT (54H GO TO JAIL, DO NOT PASS GO, DO NOT COL-
    LECT 200 DOLLARS)
15  FORMAT (54H
17  FORMAT (1H2)
18  FORMAT (8H ANSWERS)
19  FORMAT (1H0,10F11.4)
24  FORMAT (1H0)
25  FORMAT (F10.4)
26  FORMAT (8H SCALE= ,F10.4)
    READ 25,F
    PRINT 26,F
    PRINT 24
    JJ=1
    M=XSIMEQF(11,N,JJ,A,B,F,E,)
    GO TO (20,21,22),M
20  PRINT 12,F,(A(I,1),I=1,N)
    GO TO 23
21  PRINT 13
    GO TO 23
22  PRINT 14
23  GO TO 500

```

The program, when supplied with the proper input control cards, will solve simultaneous algebraic equations up to a maximum of 10 equations and 10 unknowns:

- a. When the solution is successful - BRIGHT BOY.
- b. When overflow occurs - BROKE THE BANK.
- c. When the matrix is singular - GO TO JAIL.
- d. When matrix to be inverted is not square -
(caustic comment).

A complete write-up of this FAP program can be obtained from the MIT Consultants (cc-174-3).

INPUT

Card 1 Format (I5)

This is the control card. Place a 1 in column 5.

Card 2 Format (54H _____)

Place a 1 in column 1 of the data card, then type

any comment that you wish to have printed.

Card 3 Format (I5)

The number of unknowns in the set of simultaneous equations is punched in columns 4 and 5; the units digit appearing in column 5.

Group 4 Format (5F13.4) Cards = $\frac{N \times N}{5}$

The value of the coefficients are punched five to a card. The coefficients are punched column by column (i.e., first column - all rows, second column - all rows, etc.).

Group 5 Format (5F13.4) Cards = $\frac{N}{5}$

The value of the algebraic equations are punched five per card. There is no need to fill all 5 fields on the card.

Card 6 Format (F10.4)

This value serves as a scale factor by which XSIMEQF multiplies the value of the determinant of the matrix. If the value is one, a 1.0 is punched anywhere in the above field. The scale factor is printed out in the output data as SCALE = . This scaling option applies to those who are manipulating large numbers.

Sample input and output data follow. The comment card (1st card) indicates in order: inlet pressure (psi), bypass flow (gpm), and rotational speed (rpm).

200 1.0 375

N= 5

| | | | | |
|---------|----------|----------|----------|----------|
| 576.40 | -35.00 | -10.00 | -18.40 | -513.00 |
| -35.00 | 1436.72 | -1400.00 | 0. | 0. |
| -10.00 | -1400.00 | 1420.00 | 0. | 0. |
| -18.40 | 0. | 0. | 1537.10 | -1500.00 |
| -513.00 | 0. | 0. | -1500.00 | 2529.00 |
| 505.20 | 148.00 | 860.00 | 1609.00 | 44400.00 |

ANSWERS

SCALE= 1.00

GOOD BOY DET = 3.619504E 13

| | | | | |
|-------|-------|-------|-------|-------|
| 87.86 | 87.48 | 87.47 | 86.95 | 86.95 |
|-------|-------|-------|-------|-------|

1000 0.1 150

N= 5

| | | | | |
|--------|----------|----------|----------|----------|
| 110.85 | -35.00 | -6.05 | -18.40 | -51.40 |
| -35.00 | 1436.72 | -1400.00 | 0. | 0. |
| -6.05 | -1400.00 | 1412.05 | 0. | 0. |
| -18.40 | 0. | 0. | 1537.10 | -1500.00 |
| -51.40 | 0. | 0. | -1500.00 | 1605.20 |
| 285.70 | 148.00 | 516.00 | 1609.00 | 4629.99 |

ANSWERS

SCALE= 1.00

GOOD BOY DET = 6.280575E 11

| | | | | |
|-------|-------|-------|-------|-------|
| 92.84 | 91.77 | 91.75 | 89.38 | 89.38 |
|-------|-------|-------|-------|-------|

3000 0 250

N= 5

| | | | | |
|---------|----------|----------|----------|----------|
| 54.24 | -35.00 | -0.72 | -18.40 | -0.12 |
| -35.00 | 1436.72 | -1400.00 | 0. | 0. |
| -0.72 | -1400.00 | 1401.41 | 0. | 0. |
| -18.40 | 0. | 0. | 1537.10 | -1500.00 |
| -0.12 | 0. | 0. | -1500.00 | 1502.72 |
| 1067.30 | 148.00 | 59.30 | 1609.00 | 224.00 |

ANSWERS

SCALE= 1.00

GOOD BOY DET = 3.888511E 10

| | | | | |
|--------|--------|--------|--------|--------|
| 173.80 | 168.25 | 168.21 | 126.87 | 126.80 |
|--------|--------|--------|--------|--------|

In all, ninety-one (91) data points (solution of 91 separate 5x5 matrices) were obtained utilizing this procedure. The five temperatures given in the output of this program conform respectively to the five lettered (A,B,C,D,E) nodes in Figure IX on page 14.

APPENDIX C
BIBLIOGRAPHY

1. Snapp, R.B., "An Analytical Study of Thin Fluid Films in Face-Type Shaft Seals", U. S. Naval Experimental Station, NP/9430(851), July 1962.
2. Orcutt, F.K. and H.S. Cheng, "Preliminary Analytical Investigation of Radial Face Seals", Mechanical Technology Incorporated, MTI-64TR22, MEL Sponsored Report, April 24, 1964.
3. Foster-Miller Associates, Inc., "Preliminary Investigation Leading to a Sound Analytical Understanding of Existing Face-Type Seals for Submarine Propeller shafts", MEL Sponsored Report, April 29, 1964.
4. Cheng, H.S., "On the Elastohydrodynamic Film and Pressure Profile of High-Pressure Face Seals", Mechanical Technology Incorporated, MTI-65TR3, MEL Sponsored Report, February 1, 1965.
5. Foster-Miller Associates, Inc., "Final Report on Development of a Sound Analytical Understanding of Existing Face-Type Seals for Submarine Propeller Shafts", MEL Sponsored Report 290/65, May 21, 1965.
6. Verbal communication with Mr. Watt Smith and Mr. Ralph Snapp of the U. S. Navy Marine Engineering Labor-

atory, July 1965.

7. Sastelli, K.S., Collected data from experiments with a Sealol Series 900 Step Seal, August 1965.
8. Kraus, A.D., "Heat Flow Theory", Electrical Manufacturing, p. 123-142, April 1959.

thesl4

On the thermal limitations of deep subme



3 2768 002 10235 2

DUDLEY KNOX LIBRARY